의학박사 학위논문

진행성 암에서의 신흥 바이오마커: 예후적 함의와 치료 목표로서의 잠재성

Emerging Biomarkers in Advanced Cancers: Prognostic Implications and Potential Targets for Therapy

울 산 대 학 교 대 학 원

의 학 과

김 미 정

진행성 암에서의 신흥 바이오마커: 예후적 함의와 치료 목표로서의 잠재성

지도교수 장세진, 최진

이 논문을 의학박사 학위 논문으로 제출함

2024년 8월

울 산 대 학 교 대 학 원

의 학 과

김 미 정

김미정의 의학박사학위 논문을 인준함

심사위원 김 지 훈 인

심사위원 장 세 진 인

심사위원 송 동 은 인

심사위원 강 준 인

심사위원 안 보 경 인

울 산 대 학 교 대 학 원

2024 년 8 월

Abstract

Background

The exploration of biomarkers is essential for treatment and personalized medicine in advanced cancers. This study investigated the prognostic and therapeutic implications of three emerging biomarkers: NEK9–EG5 axis in colon cancer, HER3 in *ALK*-positive non-small cell lung cancer (NSCLC), and PD-L1 expression with the tumor microenvironment (TME) of *ALK*-positive NSCLC.

Methods

For the colon cancer study, immunohistochemistry (IHC) analysis was conducted on tissue samples from 138 pT3 colon cancer patients to evaluate NEK9, EG5, and acetyl-α-tubulin expression. In the NSCLC study, IHC staining was performed on *ALK*-positive NSCLC tissue specimens before/after ALK inhibitors to assess HER3 expression, with western blot analysis used to confirm HER3 activation via the HRG1 ligand. Additionally, combination therapy effects of ALK and EGFR inhibitors were tested on *ALK*-positive NSCLC cell lines. For the PD-L1 expression and TME study in *ALK*-positive NSCLC, IHC analysis of CD3, CD4, CD8, FOXP3, and PD-1 was conducted to examine T cell subsets, and the 22C3 and SP263 assays were used for PD-L1 expression. Further, spatial transcriptomic analysis was performed on two representative *ALK*-positive NSCLC cases (one PD-L1 positive and one PD-L1 negative) to compare immune cell-related gene expression patterns.

Results

The IHC analysis of pT3 colon cancer patients revealed that NEK9 expression was significantly associated with distant metastasis (P = 0.032) and served as an independent predictive factor for metastasis (HR = 3.365, P < 0.001). The NEK9-EG5 axis was active, and simultaneous high expression of both NEK9 and EG5 was associated with mitosis in colon cancer cell lines, indicating that the NEK9–EG5 axis could predict metastatic potential in pT3 colon cancer patients. In *ALK*-positive NSCLC patients (n = 96), high HER3 expression correlated with poorer survival, especially in *EML4-ALK* variant 1/2 (V1/V2) patients and this correlation was significant in specimens collected both before and after ALK inhibitor treatment (P = 0.022 and 0.004, respectively). Western blot analysis confirmed HER3 activation through HRG1-induced expression of pHER3, pAKT, and pERK. Combining ALK and EGFR inhibitors significantly reduced receptor tyrosine kinase signaling in *ALK*-positive NSCLC cell lines. For PD-L1 expression and TME in ALK-positive NSCLCs (n = 68), the IHC study did not yield significant or explainable results regarding the relationship between T cell subsets and PD-L1. However, spatial transcriptomic analysis demonstrated minimal coexpression rates of *CD274* (encoding PD-L1) and *PDCD1* (encoding PD-1) in PD-L1 positive cases with higher *CD68* (pan-macrophages) and *CD163* (M2-like macrophages) in these coexpression spots, compared to the PD-L1 negative case. This implies that *ALK*-positive NSCLC may not involve direct contact between PD-1 receptor and PD-L1 ligand cells, potentially explaining the limited efficacy of immune checkpoint inhibitors in these patients. Notably,

CD163 expression correlated with significantly higher *CD274* levels, while *PDCD1* levels showed little difference between PD-L1 positive and negative cases. The findings suggest that higher levels of PD-L1 positive tumor-associated macrophages TAMs and relatively lower levels of PD-1 positive immune cells do not necessarily lead to immune escape of tumor cells.

Conclusions

These findings suggest that targeting the NEK9–EG5 axis, assessing HER3 expression, and understanding PD-L1 interactions in the tumor microenvironment may provide promising strategies for personalized treatment approaches in colon cancer and *ALK*-positive NSCLC.

Keywords: HER3, NEK9, PD-L1, ALK, non-small cell lung cancer, colon cancer

CONTENTS

List of Figures

Chapter 1

Chapter 2

Chapter 3

List of Tables

Chapter 1

Chapter 2

General introduction

The exploration of biomarkers from the perspectives of tumor biology is increasingly important for the treatment of advanced cancers. These biomarkers not only serve as tools for prognosis prediction but also as potential targets for innovative therapies, thus playing a crucial role in the personalized medicine. This introduction outlines the significance of three such biomarkers—each studied extensively through the lenses of tumor biology and pathology —and their implications for therapeutic strategies.

The first focus is on NEK9-EG5 axis and microtubule acetylation, which are implicated in the regulation of the mitotic spindle and microtubule dynamics. In the context of colon cancer, pathological insights into NEK9 and EG5 highlight its role in tumor progression and metastatic potential. By investigating their expression patterns and functional impact within tumor cells, these proteins might be useful for predicting metastatic potential among patients with advanced colon cancers. Researchers can identify targeted therapies that might inhibit their oncogenic activities, thereby potentially controlling disease progression.

Next, we explore HER3, a receptor tyrosine kinase in the ERBB family, within the framework of Anaplastic lymphoma kinas (*ALK*)-positive non-small cell lung cancer (NSCLC). Pathological evaluation of HER3 involves analyzing its expression and interactions with other cellular receptors that drive tumor growth and resistance mechanisms. The biology of HER3-mediated signaling pathways offers a fertile ground for developing targeted therapies that could work synergistically with ALK inhibitors, enhancing their effectiveness.

Finally, the interaction between PD-L1 expression and the tumor microenvironment in *ALK*-positive NSCLC is examined. From a pathological standpoint, the assessment of PD-L1 levels and the characterization of the immune cells within the tumor microenvironment provide critical insights into the tumor's ability to evade immune surveillance. Understanding these dynamics is key to optimizing immunotherapeutic approaches and tailoring them to individual patient profiles, potentially leading to more effective and personalized treatment plans.

Through detailed pathological and biological analysis of these biomarkers, we aim to bridge the gap between molecular insights and clinical applications, underscoring the potential of these biomarkers in managing and treating advanced cancers.

Chapter 1: Overexpression of the NEK9–EG5 axis is a novel metastatic marker in pathologic stage T3 colon cancer

1. Introduction

Colorectal cancer (CRC) is the third most prevalent cancer worldwide, comprising 8% of all adulthood malignant tumors, and is the second leading cause of cancer-related mortality (5.8% of the total deaths) [1, 2]. Despite advancements in treatment reducing CRC mortality, the 5-year relative survival rate for stage IV patients is below 15%, whereas it's 91% for T1–T3M0 and 72% for T4M0 cases. [3].

The NEK family, part of the NIMA proteins, includes 11 NEKs (NEK1-11) that exhibit cell cycle-dependent activity [4]. NEK9 regulates mitotic spindle assembly and, with NEK6 and NEK7, forms a kinase cascade where NEK9 activates NEK6/7 by phosphorylation, facilitating mitotic progression. (Fig. 1a) [5]. NEK proteins' expression varies in cancers, with NEK9's decrease linked to aggressive breast cancer, NEK7's increase to poor outcomes in gastric/pancreatic cancers, and NEK2/6 overexpression to worse colorectal cancer prognosis, necessitating research into their tissue-specific cancer roles [6-8].

NEK9 activates NEK6/7, which in turn activate EG5 (kinesin-5), forming a regulatory NEK9-EG5axis that recruits EG5 to the centrosome, controlling mitosis and microtubule polymerization (Fig. 1b) [9]. Acetylation of α-tubulin within microtubule lumens, particularly at K40, indicates stability and longevity, aiding self-repair and resistance to mechanical stress [10]. Despite the known regulatory of NEK9, EG5 and microtubule acetylation in mitotic events, few studies have investigated the prognostic significance of these factors in different tumor types. A recent study indicates that microtubule stabilization by NEK9 and NEK7 is linked to enhanced cancer cell migration and shows a correlation between NEK9 activity and the expression of acetylated tubulin. [11].

Although little is yet known about CRC metastasis specifically, tumor metastasis is generally associated with cell proliferation, motility involving an epithelial-mesenchymal transition (EMT), mitosis, and microtubule dynamics [12-14]. Here, we investigated the altered expression of NEK9, EG5, and acetyl-α-tubulin, and their correlation with the EMT-related proteins (E-cadherin, claudin-1, vimentin, and β-catenin) to evaluate their role and possible prognostic significance for metastasis in patients with pathologic T3 stage (pT3) colon cancers.

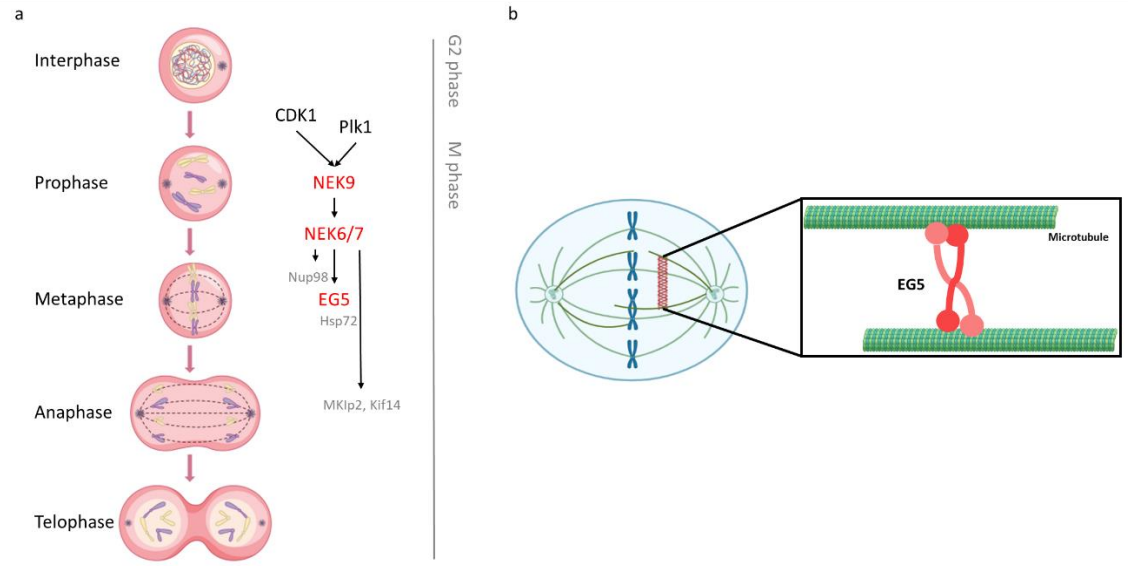

Fig. 1. Dynamics of Mitotic Progression and Microtubule Interaction by Eg5. (a) Sequential stages of mitosis from interphase to telophase, with regulatory proteins such as NEK9, NEK6/7 and Eg5. (b) Focus on the mitotic spindle during metaphase, showing centrosomes, microtubules, chromosomes, and the role of Eg5 in microtubule cross-linking.

2. Materials and methods

2.1. Patients

A cohort of 138 patients diagnosed with pT3 colon adenocarcinoma, based on the 8th edition of the American Joint Committee on Cancer (AJCC) system, between 2015 and 2017 at Asan Medical Center was enrolled. Patients who underwent a curative resection without neoadjuvant therapy were included. Medical records were reviewed to collect data on sex, age, radiologic findings, survival, and pathology, including tumor size, histologic grade, lymph node metastasis, lymphovascular invasion (LVI), perineural invasion (PNI), and tumor budding. TNM staging was applied according to the AJCC 8th edition, defining N and M categories as: N0, no lymph node metastasis; N1, 1-3 lymph nodes with metastasis or tumor deposits without lymph node involvement; N2, metastasis in 4 or more lymph nodes; M0, no distant metastasis; M1, confirmed distant metastasis.

2.2. Tissue microarrays and immunohistochemistry

Hematoxylin and eosin-stained slides of the 138 cases were reviewed by two experienced pathologists (MK and HJJ). Tissue microarrays (TMAs) were constructed from the formalin-fixed paraffin-embedded (FFPE) tissue blocks with two randomly selected tumor cores per case measuring 3 mm in diameter. Immunohistochemical (IHC) staining was performed on these TMA blocks using a Ventana BenchMark XT Autostainer (Ventana Medical Systems, Tucson, AZ) and an UltraView staining kit (Ventana). The

samples were incubated with each of the following primary antibodies: NEK9 (1:500; ab138488, Abcam, UK), EG5 (1:100; 4203, Cell Signaling Technology, Boston, MA), acetyl-α-tubulin (1:1000; 5335, Cell Signaling Technology), E-cadherin (1:200; clone 4A2C7, Zymed, CA), claudin-1 (1:100; #359A-15, Cell Marque, CA), vimentin (1:500, clone V9, Zymed), and β-catenin (1:200, clone 14, Cell Marque).

The immunostaining results were interpreted by two pathologists who scored staining intensity and proportion. Discrepancies between cores were averaged. NEK9 interpretation followed Lennartz et al., with four scoring categories: 0 (no staining), 1+ (weak ≤70% or moderate ≤30%), 2+ (weak >70% or moderate >30% to ≤70%), and 3+ (moderate >70% or strong >30%) [15]. For EG5 and acetyl-α-tubulin, scoring was: 0 (none or <10%), 1+ (faint/weak ≥10%), 2+ (weak to moderate ≥10%), 3+ (moderate to strong ≥10%). E-cadherin and claudin-1 were scored: 0 (none), 1+ (≤33%), 2+ (>33% to ≤66%), 3+ (>66%) [16]. E-cadherin and claudin-1 were scored: 0 (none), 1+ (≤33%), 2+ (>33% to ≤66%), 3+ (>66%) [17]. Vimentin expression ≥5% was high, <5% low [18, 19]. β-catenin was high if >80% cells stained, otherwise low [20]. These categories facilitated logistic regression and Pearson's correlation analyses, splitting scores into low (0-1) and high (2-3) expression subgroups for cross-analysis.

2.3. Cell culture and cell cycle analysis

Primary tumor-derived SW480 and metastasis-derived SW620 colon cancer cell lines were grown in RPMI 1640 (Invitrogen-GIBCO, Carlsbad, CA) supplemented with 10% fetal bovine serum, 50 μg penicillin/mL, and 100 μg streptomycin/mL at 37°C in a 5% CO2 incubator. Nocodazole was purchased from Sigma-Aldrich (SML1665, St. Louis, MO) and stock solutions were prepared in DMSO and stored at -20°C. Cells were treated with either DMSO or 500 nM nocodazole for 24 or 48 hours, and then released by a switch to normal media to allow re-entry into the cell cycle. For cell cycle analysis, cells were harvested and collected by centrifugation. Briefly, 5 x 105 cells were washed with ice-cold PBS, fixed in 50% ethanol (vol/vol), and treated 5 μl of a 1 mg/ml RNase A. The cells were stained with 50 μl of a 50 μg/ml propidium iodide (PI) solution for 15 minutes on ice and then subjected to flow cytometry. DNA histograms were subsequently analyzed using BD FACSCantoTM (BD Biosciences, San Jose, CA).

2.4. Western blot analysis

For western blotting, whole-cell lysates were prepared in RIPA lysis buffer (50 mM Tris-HCL [pH 8.0], 150 mM NaCl, 0.5 mM EDTA, 1 mM DTT, 0.1% NP-40, 0.1% SDS) containing a protease inhibitor cocktail (BPI-9200, Tech & InnovationTM, Bucheon, Korea) and a phosphatase inhibitor cocktail (45065; Santa Cruz, Santa Cruz, CA). Proteins were then separated on an 8% or 10% SDS-PAGE gel and transferred to polyvinylidene fluoride (PVDF) membranes using an iBlotTM dry blotting system (Invitrogen). The transferred membranes were cut after the blocking steps to analyze with different antibodies. Immunoblotting analysis were performed with the following primary antibodies: pNEK9 (T210) (1:5000, ab63553; Abcam), NEK9 (1:5000, ab138488; Abcam), EG5 (1:1000, 4203; Cell

signaling Technology), acetyl-α-tubulin (Lys40) (1:1000, T7451; Sigma-Aldrich), pAKT (S473) (1:1000, 9271; Cell signaling Technology), AKT (1:1000, 9272; Cell signaling Technology), cyclin B1 (1:1000, sc-245; Santa Cruz) and β-Actin (1:10000, 5441; Sigma-Aldrich). Rabbit or mouse horseradish peroxidase (HRP)-labelled secondary antibodies (1:10000; ENZO, Farmingdale, NY) were then used. The blots were visualized using a SuperSignal West Pico Chemiluminescent Substrate (Thermo Fisher Scientific-Pierce, Rockford, IL).

2.5. Statistical analysis

Cross-tab analysis with chi-square and Fisher's exact tests assessed the relationship between IHC expression and clinicopathological features. Overall survival (OS) was calculated from diagnosis to death or last follow-up, analyzed using Kaplan–Meier method and log-rank test. Univariate and multivariate logistic regression analyzed the association of distant metastasis in colon cancer with clinicopathologic variables, including IHC profiles. Pearson's correlation coefficients explored correlations among expression patterns. Statistical analyses were performed using SPSS version 21.0.0, with a significance threshold of $P < 0.05$.

3. Results

The study included 138 pT3 stage colon adenocarcinoma patients, of whom 51 developed distant metastasis (stage IV). The mean age was 63.6 years (range 31–90), with a nearly equal male to female ratio of 1:1.03. Survival data were available for 136 patients, with a median follow-up of 46 months (range 0–155 months). Two patients lost to follow-up had been enrolled for 18 days. One was excluded from survival analysis. Of the cohort, 38 patients died, and the mean OS was 113.73 months (95% CI: 102.80–124.66).

3.1. Expression of the NEK9-EG5 axis and clinicopathologic features

Overall, 69% (91/132), 53% (70/132), and 74% (98/132) of our present study cases showed high expression for NEK9, EG5 and acetyl-α-tubulin by IHC analyses. Representative images and details of the IHC scores are provided in Figure 2. The CRC tumors showing high NEK9 expression were preferentially distributed among patients with M1 stage tumors ($P = 0.032$). In addition, a significant correlation was observed between high NEK9 expression and a tumor size greater than 60 mm ($P = 0.046$). High EG5 expression also showed a significant association with the LVI ($P = 0.009$). The high expression of EG5 or acetyl-α-tubulin was predominantly found in the M1 group, but these results did not reach statistical significance ($P = 0.107$ and 0.111, respectively; Table 1). The EMT markers (E-cadherin, vimentin, claudin-1 and β-catenin) were not found to be significantly associated with the M1 stage in the present study cohort, but the expression of E-cadherin or β-catenin did show an association with tumor differentiation ($P = 0.037$ and 0.002, respectively; data not shown).

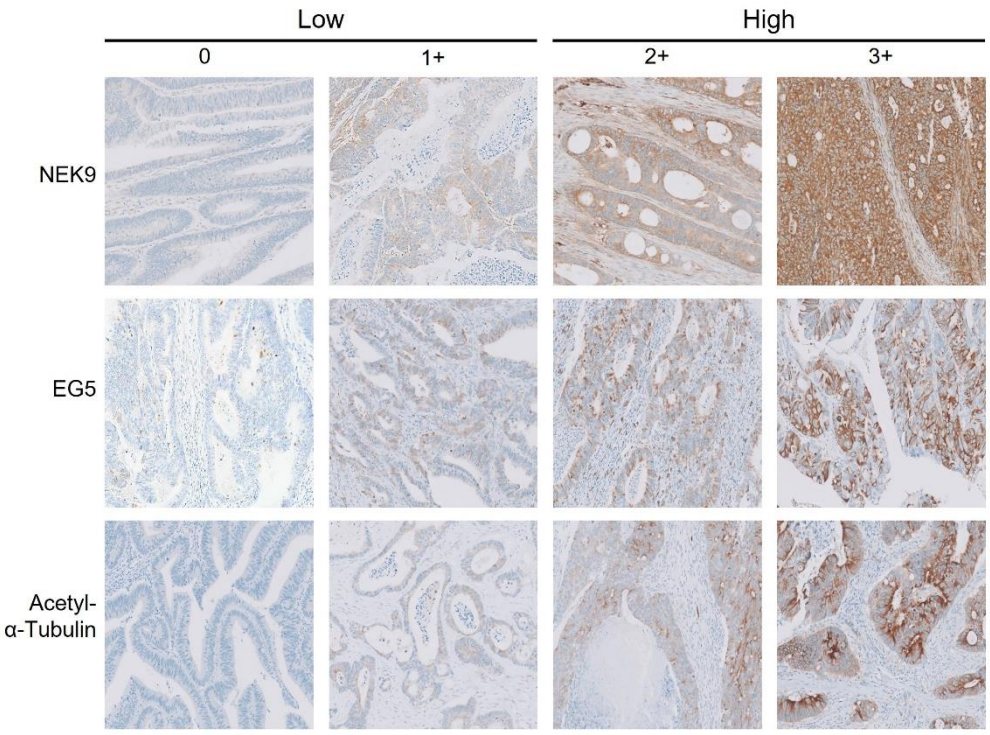

Fig. 2. Representative immunostained images of tissue microarrays from colon adenocarcinoma samples. Immunoreactivity for NEK9, EG5, and acetyl-α-tubulin is shown at 200x magnification, categorized into low (scores 0-1) and high (scores 2-3) expression groups.

Table 1. Immunohistochemical expression of NEK9, EG5 and acetyl-α-tubulin and clinicopathologic characteristics

	NEK9			EG5			Acetyl-α-tubulin		
Variables (n, %)	Low (n=41)	High (n=91)		Low (n=62)	High (n=70)		Low (n=34)	High (n=98)	
Size			0.046			0.520			0.984
≤ 60 mm	34 (82.9)	60 (65.9)		42 (67.7)	51 (72.9)		24 (70.6)	69 (70.4)	
> 60 mm	7 (17.1)	31 (34.1)		20 (32.3)	19 (27.1)		10 (29.4)	29 (29.6)	
N stage			0.767			0.996			0.989
N0	21 (51.2)	41 (45.1)		28 (45.2)	32 (45.7)		16 (47.1)	45 (45.9)	
N1	14 (34.1)	33 (36.3)		23 (37.1)	26 (37.1)		12 (35.3)	36 (36.7)	
N2	6 (14.6)	17 (18.7)		11 (17.7)	12 (17.1)		6	17 (17.3)	
M stage			0.032			0.107			0.111
M0 (stage Ⅲ)	31 (75.6)	51 (56.0)		43 (69.4)	39 (55.7)		25 (73.5)	57 (58.2)	
M1 (stage Ⅳ)	10 (24.4)	40 (44.0)		19 (30.6)	31 (44.3)		9 (26.5)	41 (41.8)	
Differentiation			0.382			0.239			0.063
WD	2 (4.9)	6 (6.6)		6 (9.7)	2 (2.9)		4 (11.6)	4 (4.1)	
MD	37 (90.2)	84 (92.3)		55 (88.7)	66 (94.3)		28 (82.4)	93 (94.9)	
PD	2 (4.9)	1 (1.1)		1 (1.6)	2 (2.9)		2 (5.9)	1 (1.0)	
LVI			0.188			0.009			0.617
Absent	24 (58.5)	42 (46.2)		38 (61.3)	27 (38.6)		18 (52.9)	47 (48.0)	
Present	17 (41.5)	49 (53.8)		24 (38.7)	43 (61.4)		16 (47.1)	51 (52.0)	
PNI			0.211			0.662			0.981
Absent	20 (48.8)	55 (60.4)		36 (58.1)	38 (54.3)		19 (55.9)	55 (56.1)	
Present	21 (51.2)	36 (39.6)		26 (41.9)	32 (45.7)		15 (44.1)	43 (43.9)	
Tumor budding			0.116			0.527			0.391
Absent	18 (54.5)	56 (70.0)		30 (62.5)	43 (68.3)		16 (59.3)	58 (68.2)	
Present	15 (45.5)	24 (30.0)		18 (37.5)	20 (31.7)		11 (40.7)	27 (31.8)	

WD, well differentiated; MD, moderately differentiated; PD, poorly differentiated; LVI, lymphovascular invasion; PNI, perineural invasion

3.2. Expression of the NEK9-EG5 axis, metastasis, and overall survival

By univariate analyses, the expression of NEK9 (hazard ratio [HR] = 2.476, 95% confidential interval [CI] 1.520 – 4.033, $P < 0.001$), claudin-1 (HR = 0.561, 95% CI 0.336 – 0.937, $P = 0.027$), the N stage (HR = 2.563; 95% CI 1.545 – 4.251, $P < 0.001$), LVI (HR = 2.971; 95% CI 1.442 – 6.122, $P = 0.003$) and the PNI (HR = 2.199; 95% CI 1.087 – 4.450, $P = 0.028$) were found to be significantly associated with distant metastasis (Table 2). Multivariate analyses revealed that NEK9 expression was the independent predictive factor for distant metastasis (HR = 3.365; 95% CI 1.786 – 6.340, $P < 0.001$), which was more significant than the N stage (HR = 2.496, 95% CI 1.284 – 4.852, $P = 0.007$), while the EMT markers (E-cadherin, vimentin, claudin-1 and β-catenin) did not show this predictive capacity with any significance (Table 2).

Kaplan-Meier survival analyses demonstrated OS differences between the low and high NEK9 expression groups, but these were not statistically significant ($P = 0.267$; Fig. 3a). Intriguingly, these different survival outcomes were similarly observed between the two groups when limited to the M0 cases (n=87) ($P = 0.338$; Fig. 3b). OS differences were also observed in relation to the EG5 and acetyl-α-tubulin expression levels among the total patient population ($P = 0.642$, and 0.764, respectively; Fig. 3c and 3d), whereas in the case of the EMT markers, only claudin-1 showed difference ($P = 0.151$; data not shown).

Table 2. Univariate and multivariate regression analysis of metastasis biomarkers in the s tudy cohort

	Variables	Metastasis		
		HR	95% CI	*P*
Univariate	Size ≥ 60 mm	0.841	0.391 – 1.806	0.657
	N stage (N2 vs N1 vs N0)	2.563	1.545 – 4.251	< 0.001
	Differentiation (PD vs MD vs WD)	0.942	0.275 – 3.226	0.924
	LVI	2.971	1.442 – 6.122	0.003
	PNI	2.199	1.087 – 4.450	0.028
	Tumor budding	0.481	0.216 – 1.072	0.073
	NEK9	2.476	1.520 – 4.033	< 0.001
	EG5	1.139	0.881 – 1.472	0.320
	Acetyl-α-tubulin	1.293	0.866 – 1.932	0.209
	E-cadherin	0.757	0.455 – 1.261	0.285
	Vimentin	0.440	0.088 – 2.210	0.319
	Claudin-1	0.561	0.336 – 0.937	0.027
	β-catenin	1.885	0.191 – 18.633	0.588
Multivariate	Size ≥ 60 mm	1.237	0.460 – 3.327	0.673
	N stage	2.496	1.284 – 4.852	0.007
	LVI	2.090	0.761 – 5.739	0.153
	PNI	1.496	0.562 – 3.983	0.420
	NEK9	3.365	1.786 – 6.340	< 0.001
	EG5	0.917	0.648 – 1.298	0.625
	Acetyl-α-tubulin	1.397	0.823 – 2.372	0.216
	E-cadherin	0.537	0.266 – 1.087	0.084
	Vimentin	0.335	0.05 – 1.912	0.218
	Claudin-1	0.554	0.286 – 1.073	0.080
	β-catenin	2.156	0.110 – 42.298	0.613

WD, well differentiated; MD, moderately differentiated; PD, poorly differentiated; LVI, lymphovascular invasion; PNI, perineural invasion

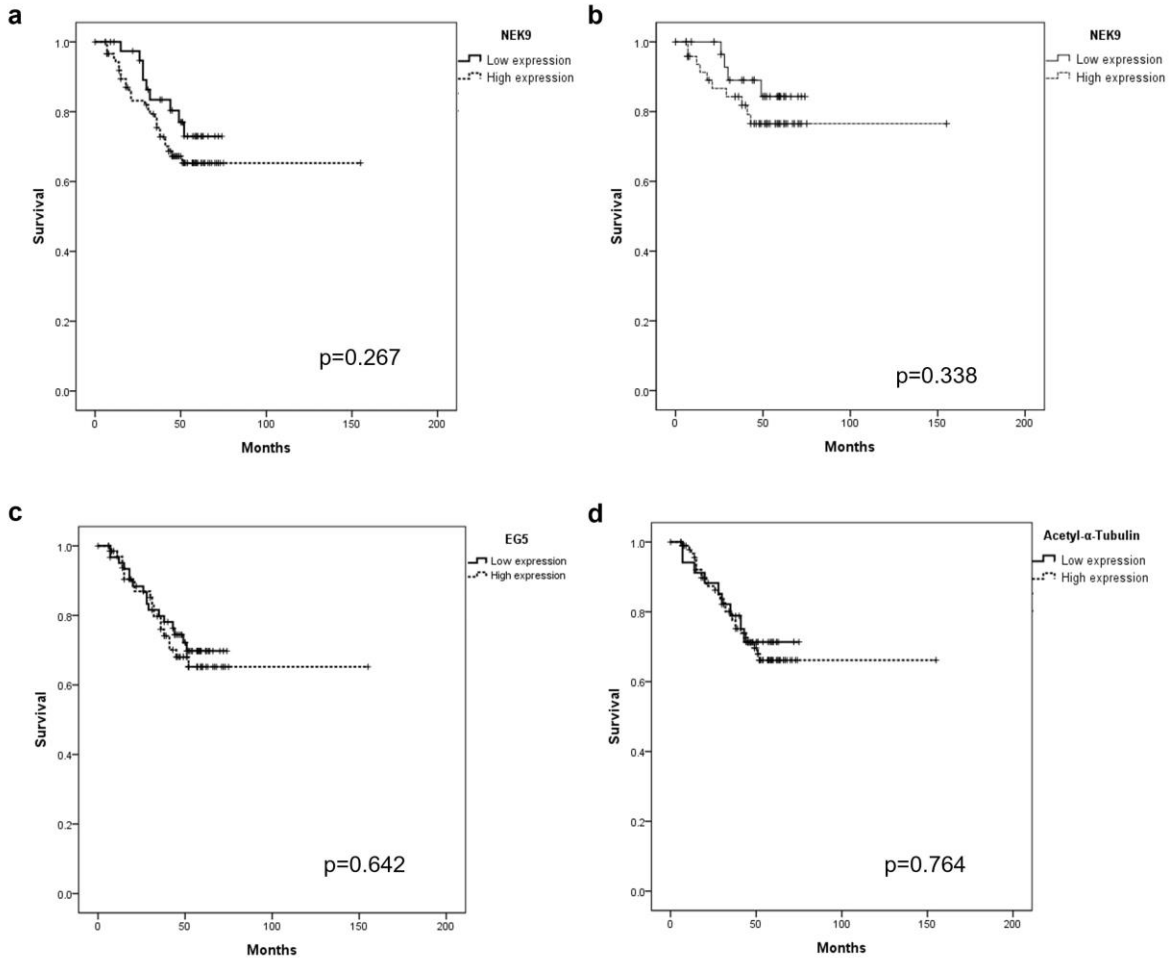

Fig. 3. Kaplan-Meier survival curves for overall survival (OS) according to the expression of NEK9, EG5 or acetyl-α-tubulin. (a) NEK9 expression in the whole cohort (n=136). (b) NEK9 expression in the M0 patient subgroup (stage III; n=87). (c) EG5 expression in the whole cohort. (d) Acetyl-α-tubulin expression in the whole cohort. OS differences were observed between the low- and high-expression cases for these proteins, with a more distinct difference for NEK9. M0, patients with no evidence of metastasis.

3.3. Immunohistochemical correlations and activity of the NEK9-EG5 axis in colon cancer cell lines

Using a Pearson's test, a significant positive correlation was found between NEK9 and EG5, and between NEK9 and acetyl-α-tubulin (r = 0.236 and P = 0.007; r = 0.181 and P = 0.038, respectively). Among the M1 stage subgroup of 51 patients, NEK9 and EG5 showed a significant positive correlation (r =0.350 and P = 0.013) and EG5 and acetyl-α-tubulin also did so with marginal significance (r = 0.276 and P = 0.053; Table 3).

Considering that NEK9, EG5, and acetyl-α-tubulin are key cell cycle proteins controlling the G2 to M phase transition, we further confirmed their concomitant expression in cell lines. SW480 and SW620 colon cancer cells were arrested at the G2/M border by 48 h of nocodazole treatment and then released to enter mitosis [21, 22]. SW480 cells passed transitioned from G2/M to G1 more rapidly than SW620 cells after this nocodazole release (Fig. 4a). The levels of cyclin B1, active NEK9 (pNEKT210) and EG5 were concordantly accumulated at the G2/M phase by nocodazole treatment and decreased when the cells were released into G1 (Fig. 4b). By contrast, the acetylated-α-tubulin and pAKTS473 levels were simultaneously decreased at the G2/M phase in which microtubule depolymerization and subsequent chromosome segregation occur. These data suggest that the NEK9-EG5 axis is active, and that the simultaneous high expression of NEK9 and EG5 is required for mitosis in colon cancer cells.

Table 3. Correlation between NEK9, EG5, and acetyl-α-tubulin immunostaining in the stud y cohort

	Total (n=138)		M1 (stage Ⅲ; n=51)		M0 (stage Ⅳ; n=87)	
Immunohistochemistry	**r**	***P***	**r**	***P***	**r**	***P***
NEK9-EG5	0.236	0.007	0.350	0.013	0.146	0.197
NEK9- Acetyl-α tubulin	0.181	0.038	0.155	0.283	0.156	0.165
EG5- Acetyl-α tubulin	0.154	0.079	0.276	0.053	0.085	0.452

M1,patients with distant metastasis; M0, patients with no evidence of distant metastasis

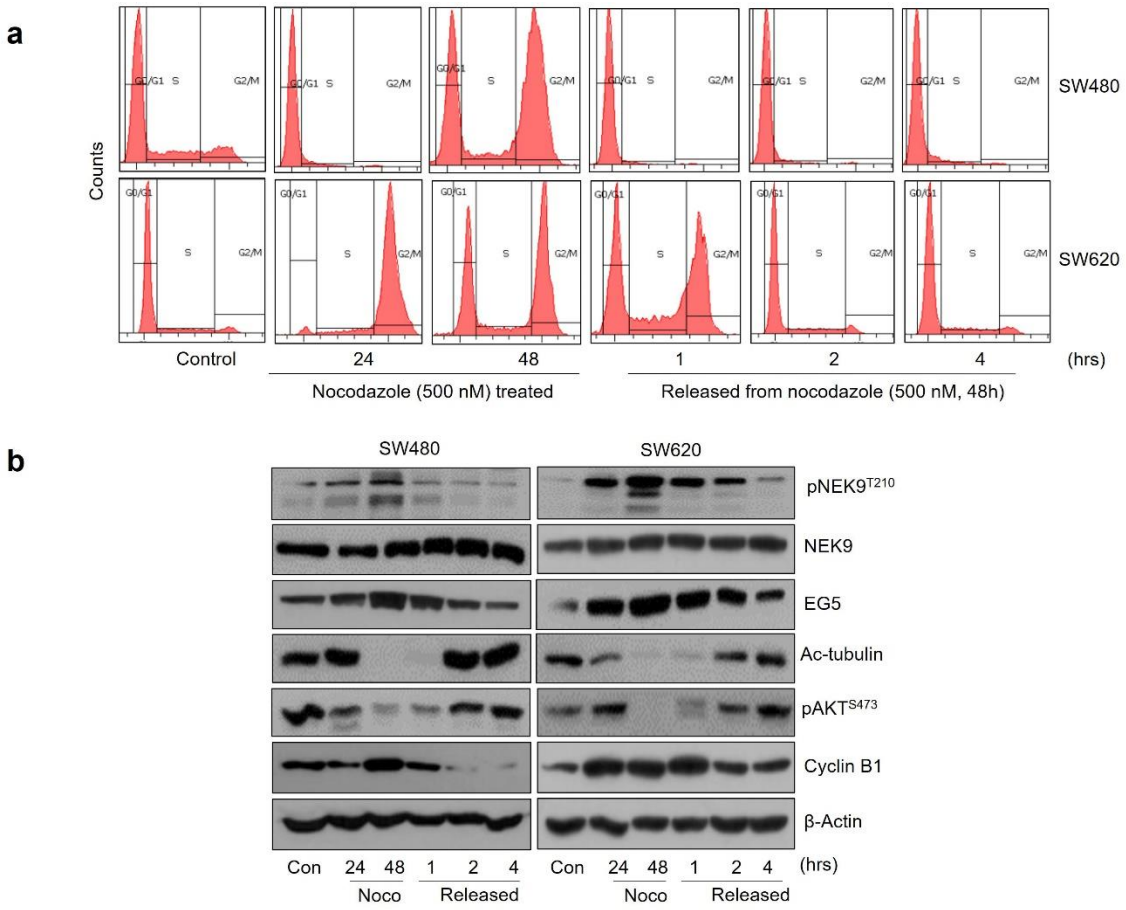

Fig. 4. Concordant expression of the NEK9-G5 axis during the G2/M phase of the cell cycle. (a) Cell cycle distribution of SW480 and SW620 colon cancer cells treated with nocodazole (500 nM) for 24 or 48 hours and then released from this block. (b) Western blot analysis of phosphorylated NKE9 (pNEK9T210), NEK9, EG5, acetyl-tubulin, phosphorylated AKT (pAKTS473) and cyclin B1 at the indicated times of nocodazole–induced G2/M arrest, and after the release from this block.

4. Discussion

In this study, we have demonstrated that, NEK9 overexpression was found to be an independent prognostic indicator of distant metastasis and might be a superior marker to the EMT proteins. Moreover, the poor OS tendency in the high NEK9 group was also found in the M0 patient subgroup (Fig. 3b), indicating that NEK9 overexpression may have a crucial role in the onset of distant metastasis in colon cancer.

Kurioka et al. showed that high NEK9 expression is associated with a poor prognosis in patients with non-small cell lung cancers lacking a functional p53, suggesting that this expression promotes tumor growth [23]. O'Regan et al. reported that NEK9 overexpression was associated with poor progression-free survival in patients with EML4-ALK lung cancer, and that this expression may have high metastatic potential [11]. In another recent study by Lu et al., a simultaneous elevation of the levels of NEK9, GP130 and p-STAT3 in the lymph nodes was associated with distant metastasis and a reduced OS outcome in gastric cancer [24]. Taken together, these findings have suggested that the aberrant expression of NEK9 is frequently observed in various cancers and is potentially a negative prognostic indicator.

A number of studies have suggested that acetylated microtubules are stable and long-lived microtubules which are consequences of microtubule acetylation [25]. There are several reports showing concordant activation of the NEK9-EG5 axis in the mitotic phase of the cell cycle [26, 27]. Our present data demonstrated that NEK9 and EG5, and NEK9 and acetyl-α-tubulin, have a positive expression correlation. Moreover, these relationships were found to be more distinct in the M1 group than among the M0 cases in our study cohort. Based on these data, we have found that an aberrant hyper-activation of the NEK9-EG5 axis, as well as stable acetylated microtubules, confer an increased metastatic potential in colon cancer. Multiple prior studies have shown that EG5 or acetyl-α-tubulin overexpression is associated with a poor prognosis [26, 28, 29]. Indeed, although the results did not reach statistical significance, we also observed that high NEK9, EG5, and acetyl-α-tubulin expression were associated with a poor OS outcome, with a more obvious tendency in the M0 group, i.e., stage III with high NEK expression. Hence, we conclude that the NEK9-EG5 axis could play a functional role in tumor cell proliferation and distant metastasis.

Our western blot analysis demonstrated that the NEK9-EG5 axis is crucial for the G2/M transition in colon cancer cells, with synchronized expression levels necessary for effective mitosis. Concordant NEK9 and EG5 accumulation at the G2/M phase by nocodazole treatment were verified in our colon cancer cell lines. However, we observed a marked decrease in acetyl-α-tubulin at the G2/M phase, whereas expression of the NEK9-EG5 axis showed an inverse relationship with acetyl-α-tubulin. We believe that G2/M synchronized cancer cells are primed for microtubule depolymerization for mitosis, and then acetylation of microtubules occurs right after mitosis to recover their structural integrity. This

finding has not been described in earlier studies and the detailed mechanisms of tubulin acetylation during mitosis require further characterization [30, 31].

5. Conclusion

In this study, we showed that high NEK9 expression could be an independent metastatic marker in colon cancer, and aberrant expression of the NEK9-EG5 axis had a role in microtubule assembly with acetylation during the tumorigenic process. Mitotic phase- and microtubule acetylation-specific proteins could be included as components of the mechanisms underlying metastasis, migration and invasiveness of tumor cells.

Chapter 2: HER3 overexpression: a predictive marker for poor prognosis in advanced *ALK*-positive non-small cell lung cancer treated with ALK inhibitors

1. Introduction

Anaplastic lymphoma kinase (*ALK*)-rearrangement has been detected in approximately 5% of patients with non-small cell lung cancer (NSCLC) [32]. The most common fusion partner in *ALK*-rearranged NSCLC is echinoderm microtubule-associated protein-like 4 (EML4), and multiple variants of EML4-ALK fusion have been reported. As a driver mutation, *EML4-ALK* fusion induces aberrant activation of ALK kinase and its downstream signaling pathways (e.g., PI3K/AKT, RAS/ERK, and JAK/STAT) resulting in cellular proliferation and tumorigenesis [33]. Following the introduction of the first-generation ALK-targeted tyrosine kinase inhibitor (TKI) crizotinib, several other ALK-TKIs, such as ceritinib, alectinib, brigatinib (second generation), and lorlatinib (third-generation), have been developed to improve overall survival (OS) [34, 35]. Nevertheless, it is important to note that the development of acquired resistance to ALK-TKIs remains a nearly inevitable challenge.

Several resistance mechanisms have been identified, including mutations within the *ALK* kinase domain and activation of ALK-independent bypass signaling pathways (Fig. 1) [36-39]. While ALK-independent resistance mechanisms are still not fully understood, MET activation, a well-known bypass pathway in *EGFR*-mutant NSCLC, has recently gained attention as a potential resistance mechanism, especially in the context of *ALK*-positive NSCLC [40]. In contrast to MET, the involvement of ERBB family members, such as EGFR, HER2, HER3, and HER4, in mediating resistance in *ALK*-positive NSCLC, remains relatively unexplored. Recent studies have shown that ALK inhibitor-resistant cell lines exhibit overexpression of phospho-EGFR or phospho-HER3, indicating their potential role in conferring resistance to ALK-TKIs [36, 41]. However, it remains unclear whether the activation of these alternative receptor tyrosine kinases (RTKs) in *ALK*-positive NSCLC affects the clinical outcomes of crizotinib, second-, or third-generation ALK-TKIs. In addition, multiple studies have focused on the activation status of RTKs after treatment with ALK inhibitors, whereas little is known about the prognostic significance of pre-existing activation of RTKs before ALK-TKI treatment.

We have comprehensively evaluated the expression of multiple RTKs, including c-MET and ERBB family members, in NSCLC tumors (the primary tumor obtained at initial diagnosis and the secondary tumor after ALK-TKI treatment) and assessed their prognostic significance in patients with NSCLC treated with ALK inhibitors. To explore other therapeutic strategies, we further investigated the treatment efficacy of a combination of ALK and EGFR inhibitors in an in vitro system with ERBB family activation.

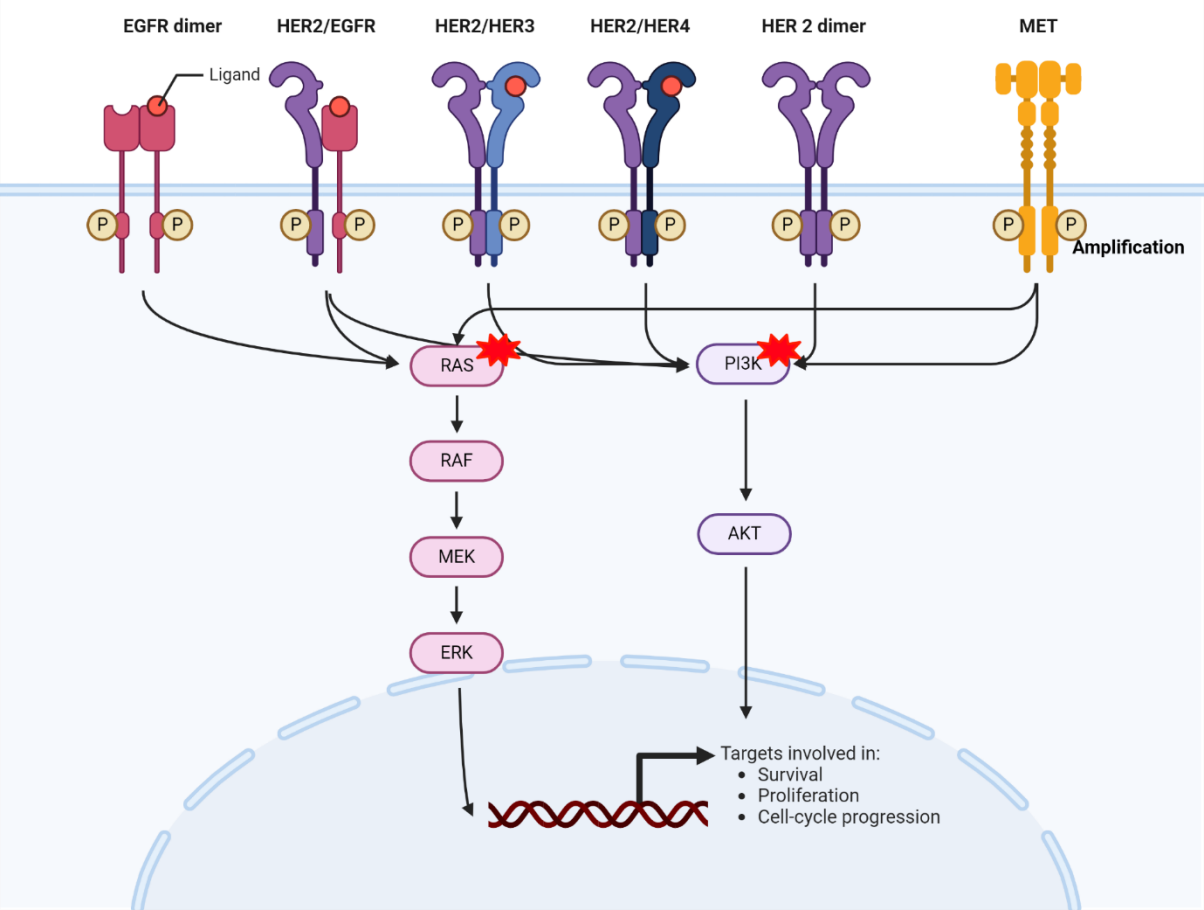

Fig. 1. Mechanisms of ALK-independent resistance to ALK inhibitors. The diagram displays alternative signaling pathways contributing to ALK-independent resistance to ALK inhibitors, involving receptor tyrosine kinases and downstream molecules that foster cell survival, proliferation, and cell-cycle progression despite ALK inhibition.

2. Materials and methods

2.1. Study cohort

We retrospectively collected consecutive cases with ALK-positive advanced-stage NSCLC (stage III or IV) between 2011 and 2021 in Asan Medical Center. All cases were pathologically confirmed as *ALK*-positive NSCLC by ALK D5F3 immunohistochemistry, *ALK* fluorescent in situ hybridization (FISH) analysis using a break-apart probe specific for the *ALK* locus (Vysis LSI ALK dual-color, break-apart rearrangement probe; Abbott Molecular, IL, USA), or clinically targeted next-generation sequencing (NGS) using the MiSeq platform (Illumina) with OncoPanel AMC version 3 [42-45]. Medical records from the patients were reviewed and data regarding demographics, Eastern Cooperative Oncology Group

(ECOG) performance status, smoking status, radiologic findings, pathologic diagnoses, molecular test results, treatment modality, and clinical follow-up were extracted. The study was conducted in accordance with the Declaration of Helsinki (as revised in 2013) and was approved by the Institutional Review Board of Asan Medical Center (IRB No. 2020-1692).

2.2. Tissue specimens and immunohistochemistry

We categorized the tissue specimens as primary tumors obtained at initial diagnosis and secondary tumors obtained after ALK-TKI treatment. All tumor cells in whole hematoxylin and eosin-stained slides were evaluated. Formalin-fixed, paraffin-embedded tissue sections (5 μm thick) were stained using an automatic device (Benchmark XT; Ventana Medical Systems, Tucson, AZ, USA) as per the manufacturer's protocol [46]. Immunohistochemical (IHC) staining was performed on whole slides using a fully automated IHC assay on a Ventana BenchMark XT Autostainer (Ventana Medical Systems, RI, USA). The specimens were incubated with antibodies against c-MET (1:400; #257261, DAKO, Glostrup, Denmark), EGFR (1:200; 31G7, Zymed, CA), HER2 (1:200; 4B5, Ventana Medical System, Tucson, AZ), and HER3 (1:50; D22C5, Cell Signaling Technology, Boston, MA).

In the IHC analysis, c-MET and EGFR staining was scored as follows: 0 for no staining, 1+ for faint/partial, 2+ for weak/complete in >10% of cells, and 3+ for intense/complete in >10% of cells. Scores of 0-2+ indicated low expression, while 3+ indicated high expression [47, 48]. For HER2 and HER3 IHC analysis: 0 indicated no staining or ≤10% of cells stained; 1+ was faint/barely perceptible staining in >10% of cells; 2+ represented weak/moderate complete staining in >10% of cells; and 3+ signified strong/complete staining in >10% of cells. Scores 0-1+ were categorized as low expression, and 2-3+ as high expression [49-51].

2.3. Cell lines and cultures

The human ALK-positive NSCLC cell lines, H3122 (*EML4-ALK* variant 1; V1) and H2228 (*EML4-ALK* variant 3a/b; V3), were grown in RPMI 1640 (Invitrogen-GIBCO, Carlsbad, CA) supplemented with 10% fetal bovine serum, 50 μg penicillin/mL, and 100 μg streptomycin/mL at 37°C in a 5% CO2 incubator. Heregulin 1 (HRG1) was purchased from Prospec (cyt-733; Ness-Ziona, Israel) and stock solutions were prepared in DMSO. Lorlatinib (S7536) and erlotinib (S7786) were purchased from Selleckchem (Houston, TX).

2.4. Western blot analyses

Cells were treated with either DMSO (10 nM HRG1 for 4 hours) followed by lorlatinib (3.12 nM), erlotinib (5 μM), or a combination of lorlatinib and erlotinib for 2 hours in the presence of HRG1. The selected doses of the drugs were the IC50 values determined by the CellTiter-Glo® Luminescent Cell Viability Assay (Promega, Madison, WI) in H3122 cells. Whole-cell lysates were prepared in RIPA lysis buffer (50 mM Tris-HCL [pH 8.0], 150 mM NaCl, 0.5 mM EDTA, 1 mM DTT, 0.1% NP-40, and 0.1% SDS)

containing a protease inhibitor cocktail (BPI-9200, Tech & InnovationTM, Bucheon, Korea) and a phosphatase inhibitor cocktail (45065; Santa Cruz, Santa Cruz, CA). Proteins were separated on an 8% or 10% SDS-PAGE gel and transferred to polyvinylidene fluoride (PVDF) membranes using an iBlotTM dry blotting system (Invitrogen). Immunoblotting analyses were performed with anti-phospho-ALK (Y1604) (3341; Cell Signaling Technology, Beverly, MA), anti-ALK (3791; Cell Signaling Technology), anti-phospho-HER3 (Y1289) (4791; Cell Signaling Technology), anti-HER3 (M7297; DAKO), anti-phospho-HER2 (Y1248) (BS4090; Bioworld technology, St. Louis Park, MN), anti-HER2 (A0485; DAKO), anti-phospho-MET (Y1234/1235) (3077 Cell Signaling Technology), anti-MET (4560; Cell Signaling Technology), anti-phospho-AKT (S473) (9271; Cell Signaling Technology), anti-AKT (9272; Cell Signaling Technology), anti-phospho-Erk (T202/Y204) (9101; Cell Signaling Technology), anti-Erk (9102; Cell Signaling Technology), anti-phospho-Myc (S62) (ab185656; Abcam, Cambridge, U.K), anti-Myc (ab39688; Abcam), and anti-β-actin (A5441; Sigma, St. Louis, MO) antibodies and visualized using the SuperSignal West Pico Chemiluminescent Substrate (34080; Pierce, Rockford, IL).

2.5. Statistical analysis

The 5-year OS was determined using Kaplan–Meier analysis, with the log-rank test evaluating survival differences. OS was measured from diagnosis to death or last follow-up, censoring living patients. The expression of c-MET, EGFR, HER2, and HER3, related to *EML4-ALK* variants in tumors, was analyzed via X^2 or Fisher's tests. Statistical procedures used SPSS version 21.0.0 and R version 4.2.1, considering a P-value < 0.05 as significant.

3. Results

3.1. Baseline characteristics

A total of 104 patients were included in our study based on the inclusion criteria; however, eight patients, who were lost to follow-up or not treated with ALK inhibitors, were excluded. Thus, 96 patients were finally enrolled and their baseline characteristics are summarized in Table 1. Eight (8.3%) patients had prior surgery for the disease and subsequently received ALK inhibitor(s) for disease progression. For the IHC analysis, 24 out of 96 cases (patients) were excluded due to limited tissue availability. Therefore, we performed the IHC analysis on the remaining 72 cases, and the number of primary and secondary tissue specimens analyzed is presented in Figure 2. At the last follow-up, among the 72 patients, 19 (40.3%) patients were receiving crizotinib, while second-generation ALK inhibitors (ceritinib, alectinib, or brigatinib) were being administered to 37 (51.4%) patients, while 6 (8.3%) patients received the third-generation inhibitor lorlatinib. Among the 43 patients not on crizotinib, 22 were receiving second-line ALK-TKIs after crizotinib, while the remaining patients were receiving them as first-line ALK-TKIs.

Table 1. Baseline characteristics of patients with *ALK*-positive advanced non-small cell lung cancer

Variables	Patients, *N* (%)
Age, median (range), years	54.5 (53–78)
Sex	
Male	47 (49.0)
Female	49 (51.0)
Smoking history	
Current	14 (14.6)
Former	18 (18.8)
Never	64 (66.7)
ECOG performance status	
0	12 (16.4)
1	59 (80.8)
2	2 (2.7)
Pathologic diagnosis	
Adenocarcinoma	93 (96.9)
Other[a]	3 (3.1)
Brain metastasis	
Present	59 (62.8)
Absent	35 (37.2)
EML4-ALK fusion variant	
V1	27 (37.0)
V2	10 (13.7)
V3a/b	33 (45.2)
V5	2 (2.7)
V7	1 (1.4)
Prior lines of therapy before ALK inhibitor	
0	54 (56.3)
1	34 (35.4)
2	6 (6.3)
≥3	2 (2.1)
Prior platinum-based therapy	
Present	40 (41.7)
Absent	56 (58.3)
Total	**96 (100)**[b]

[a]Includes large cell neuroendocrine carcinoma, squamous cell carcinoma, and non-small cell carcinoma,

not-otherwise specified. [b]Some variables did not reach 96 due to the non-availability of data. ECOG, Eastern Cooperative Oncology Group.

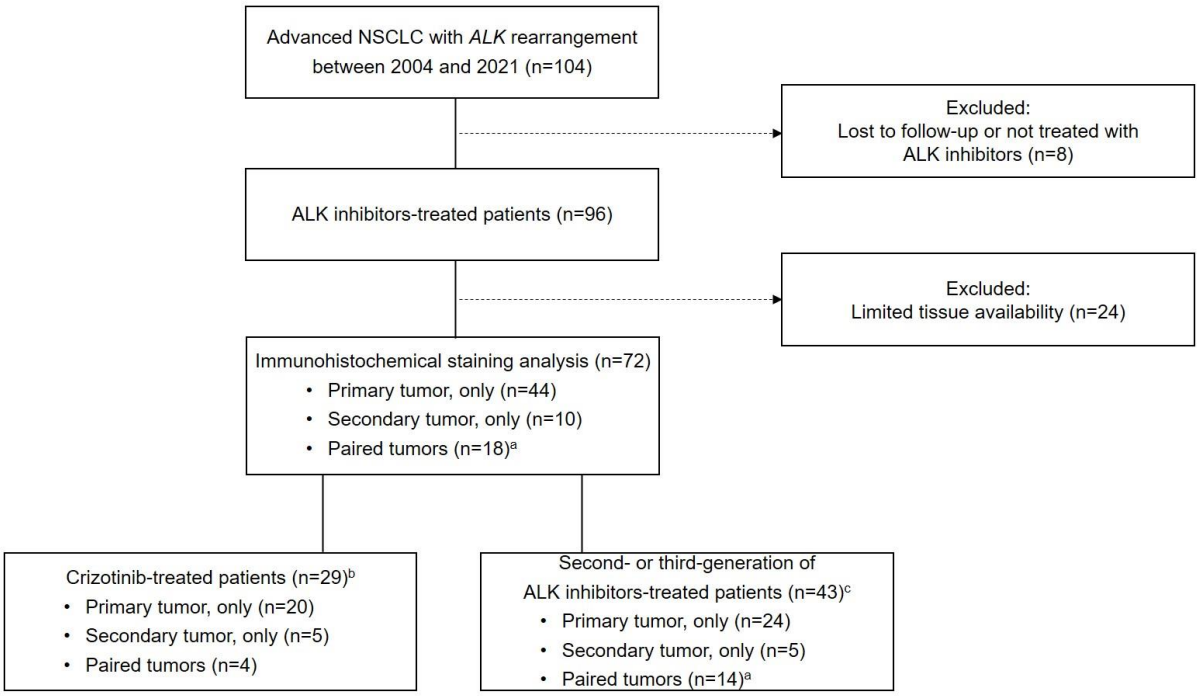

Fig. 2. Flow diagram of the cohort selection.
aOne patient was additionally excluded due to limited tissue availability for the c-MET and EGFR analysis. bPatients who received crizotinib without further generations of ALK inhibitors during the follow-up. cPatients who received second- or third generation ALK inhibitors as any line of therapy during the follow-up. NSCLC, non-small cell carcinoma.

3.2. Overexpression of c-MET, EGFR, HER2, and HER3 before/after ALK inhibitor treatment

Of the tissue specimens collected from the 72 patients, 62 were primary tumors (44 from primary tumors only and 18 from paired tumors), and 28 were secondary tumors (10 from secondary tumors only and 18 from paired tumors) (Fig. 2). From 72 patients, 62 primary tumors and 28 secondary tumors were collected; one primary and one secondary specimen were excluded from c-MET and EGFR analysis due to insufficient tissue. The IHC staining results, as depicted in Figure 3a, showed high expression of c-MET in 4.9% and EGFR in 18.0% of primary tumors, and in secondary tumors, 18.5% and 37.0%, respectively. For HER2 and HER3, high expression was 1.6% and 25.8% in primary tumors, and 10.7% and 35.7% in secondary tumors.

Secondary tumors generally displayed higher receptor tyrosine kinase expression compared to primary tumors (Fig. 3b). There was a notable increase in c-MET expression post-ALK inhibitor

treatment, and a subset of ALK inhibitor-naïve patients showed high primary tumor expression of EGFR or HER3, indicating intrinsic heterogeneity in *ALK*-positive NSCLC ERBB family expression. These percentages are not derived from paired case comparisons but instead from the total number of primary and secondary specimens. In paired analyses, low-expression primary tumors showed increased high-expression rates in secondary tumors: 11.8% for c-MET, 40% for EGFR, 17.6% for HER2, and 21.4% for HER3. However, these comparisons lacked statistical significance due to the small number of high-expression cases.

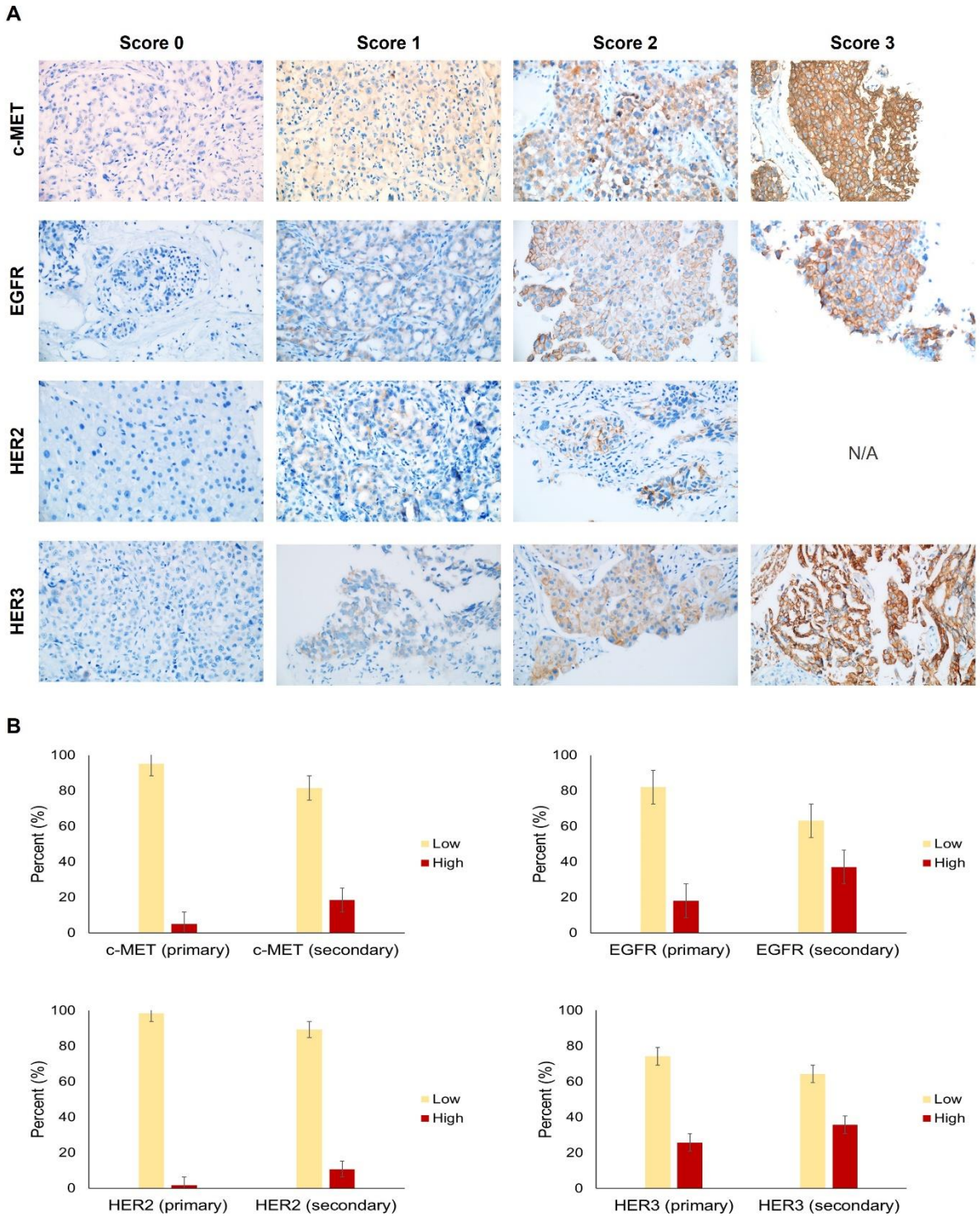

Fig. 3. Expression of c-MET, EGFR, HER2, and HER3 in ALK-positive non-small cell lung cancers. Representative immunohistochemistry images (magnification x400) with scoring (A). For c-MET and EGFR, scores 0, 1, and 2 were low expression, while a score of 3 indicated high expression. For HER2 and HER3, scores 0 and 1 represented low expression, while scores 2 and 3 were high expression. Proportion of low and high expression in primary (n=61) and secondary (n=62) tumor

specimens (B). High expression rates in primary tumors were 4.9% for c-MET, 18.0% for EGFR, 1.6% for HER2, and 25.8% for HER3. In secondary tumors, high expression rates were 18.5% for c-MET, 37.0% for EGFR, 10.7% for HER2, and 35.7% for HER3. N/A, not applicable.

3.3. Survival outcome with primary and secondary expression of c-MET, EGFR, HER2, and HER3

The median duration of follow-up was 30 months (range, 0.8–228) and the median 5-year OS was 52 months (95% CI, 34.4–69.6). The median time interval between the initial diagnosis and the first application of ALK inhibitors was 2 months (range, 0–154). Secondary tumor specimens were collected post-ALK-TKI therapy, with a median interval of 17 months between ALK-TKI initiation and second biopsy (range, 3 to 71 months). With the introduction of second- and third-generation ALK inhibitors, crizotinib is less used as a first-line therapy. We divided patients into two groups for survival analysis: those treated with second- or third-generation ALK-TKIs (n = 43), and those receiving only crizotinib (n = 29). No significant survival differences were noted based on c-MET, EGFR, or HER3 expression levels in primary tumors, although trends toward poorer outcomes were observed for high EGFR and HER3 expressions (Fig. 4a – 4c). In secondary tumors, high c-MET expression correlated with worse survival (P = 0.008; Fig. 4d). The analysis did not find significant survival differences for high expression of EGFR, HER2, and HER3 in secondary tumors (Fig. 4e – 4g), nor did it show significant findings in the crizotinib group due to limited events.

Further analysis examined RTK expression in the V1/V2 subgroup showed a non-significant survival difference between high and low EGFR expression in primary tumors (Fig. 4h). Notably, high HER3 expression in primary tumors was associated with significantly worse OS compared to low expression (P = 0.022; Fig. 4i). However, in the V3 subgroup, no significant survival difference was observed with primary HER3 expression. In secondary tumors, high expression of c-MET, EGFR, and HER2 did not show a significant association with survival (Fig. 4j, 4k, 4l). Interestingly, the V1/V2 group with high HER3 expression exhibited a significantly poor outcome (P = 0.004; Fig. 4m). The distribution of RTK expression among the variants, including 1st to 3rd-generation ALK inhibitors, is summarized in Table 2. The proportions of low and high expression of RTK were not significantly different between V1/V2 and V3 in both primary and secondary tissues.

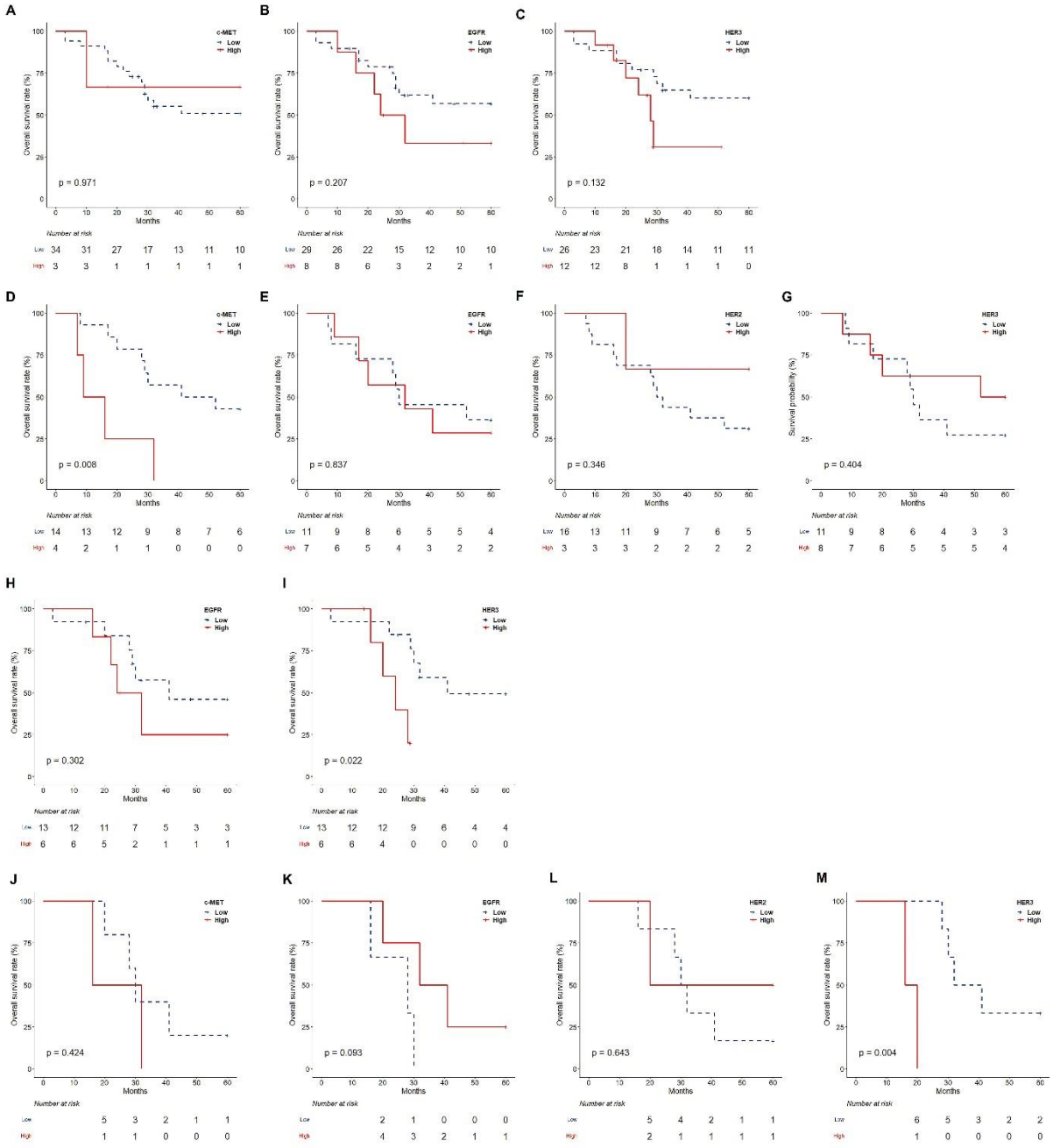

Fig. 4. Kaplan–Meier survival plots of 5-year overall survival in ALK-positive non-small cell lung cancer patients treated with second- or third-generation ALK inhibitors. The log-rank tests compared high and low expression levels of c-MET, EGFR, and HER3 in primary tumors (A, B, and C, respectively) and those of c-MET, EGFR, HER2, and HER3 in secondary tumors (D–G). In the variant 1/2 subgroup, log-rank tests compared high and low expression levels of EGFR and HER3 (H and I, respectively) in primary tumors and those of c-MET, EGFR, HER2, and HER3 in secondary tumors (J–M).

Table 2. *EML4-ALK* variant and immunohistochemical staining results of c-MET, EGFR, HER2, and HER3

Immunohistochemistry		*EML4-ALK* variant, n (%)		*P*
		V1/V2	V3a/b	
Primary tissue				
c-MET	High	0 (0)	2 (100)	0.079
	Low	28 (62.2)	17 (37.8)	
EGFR	High	8 (80.0)	2 (20.0)	0.138
	Low	20 (54.1)	17 (45.9)	
HER2	High	1 (100.0)	0 (0)	0.405
	Low	27 (58.7)	19 (41.3)	
HER3	High	8 (53.3)	7 (46.7)	0.551
	Low	20 (62.5)	12 (37.5)	
Total		28 (100)	19 (100)	
Secondary tissue				
c-MET	High	3 (75.0)	1 (25.0)	0.190
	Low	7 (38.9)	11(61.1)	
EGFR	High	4 (40.0)	6 (60.0)	0.639
	Low	6 (50.0)	6 (50.0)	
HER2	High	2 (100.0)	0 (0)	0.122
	Low	9 (42.9)	12 (57.1)	
HER3	High	3 (36.5)	5 (62.5)	0.469
	Low	8 (53.3)	7 (46.7)	
Total		10 (100)[a]	12 (100)	
		11 (100)[b]		

[a]c-MET and EGFR; [b]HER2 and HER3

3.4. Heregulin1-induced expression of receptor tyrosine kinases in EML4-ALK variant-expressing cell lines

To evaluate whether HER3 expression plays a role in ALK-positive NSCLC cell lines, we investigated multiple RTK activations in H3122 (*EML4-ALK* V1) and H2228 (*EML4-ALK* V3) after treatment with a HER3 ligand, HRG1. HER3 activation significantly increased HER2 and c-MET activity together with their major downstream signaling pathways, such as MAPK/ERK and AKT. Unexpectedly, HER3 activation strongly induced ALK activation in both cell lines (Fig. 5). Lorlatinib decreased the activity of

AKT and its downstream effector, Myc, in those cells.

Considering that *EML4-ALK* V3 is significantly associated with a higher incidence of ALK resistance mutations, the failure of lorlatinib to suppress ERK, c-MET, HER2, and HER3 activity in H2228 cells is noticeable [52]. Erlotinib, an EGFR-TKI, caused only a slight decrease in RTK activity and did not efficiently suppress ALK activity. However, the combination of lorlatinib and erlotinib significantly reduced the activities of these RTKs and Myc activity relative to lorlatinib or erlotinib alone.

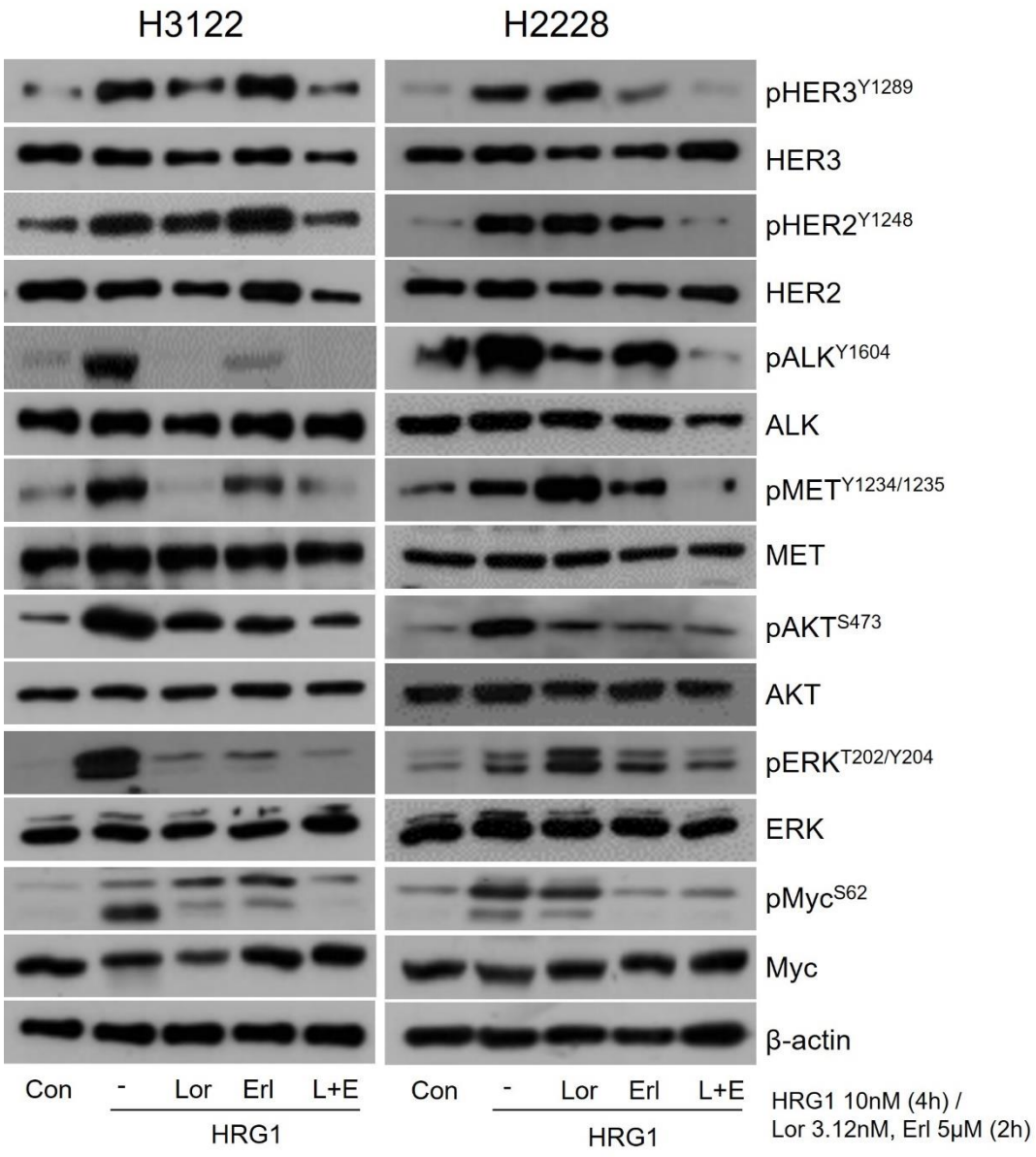

Fig. 5. Kinase activation by HRG1 and inhibitor response in EML4-ALK variant cell lines. The activation of multiple kinases, including HER3, induced by heregulin1 (HRG1) treatment, and the effects of ALK- or EGFR-tyrosine kinase inhibitors in H3122 (*EML4-ALK* variant 1) and H2228 (*EML4-ALK*

variant 3a/b) cell lines. Cells were pre-treated with HRG1 (10 nM) for 4 hours followed by lorlatinib (Lor), Erlotinib (Erl), or a combination of both for 2 hours.

4. Discussion

In this study, we assessed RTK expression, including c-MET and ERBB family members, in *ALK*-positive NSCLC across primary tumors at diagnosis and secondary tumors post-ALK-TKI therapy. Our findings indicate that EGFR or HER3 overexpression in primary tumors correlates with poorer outcomes following ALK inhibitor treatment. In secondary tumors, c-MET overexpression was associated with reduced overall survival, aligning with previous studies [39, 40]. Notably, HER3 overexpression was a significant prognostic marker in the *EML4-ALK* V1/V2 subgroup. We also observed that cells with V1 or V3 variants activated multiple RTKs, including ALK, upon HER3 ligand exposure, with significant suppression following combined ALK- and EGFR-inhibitor treatment. These results highlight the prognostic value of HER3 overexpression in predicting responses to ALK inhibitor therapy in NSCLC.

In western blot analysis, HRG1 significantly induced phospho-HER3, phospho-AKT, and phospho-ERK expression, confirming its role in activating HER3. Several studies have linked increased HRG1 or HER3 expression to resistance in NSCLC cell lines treated with crizotinib or alectinib. [36, 39, 53-56]. Our study observed HER3 overexpression in 25.8% of primary tumors, which correlated with poorer survival trends (P = 0.132) in patients treated with second- or third-generation ALK-TKIs, a correlation not seen in secondary tumors. This difference may be attributed to the dynamics of HER3 signaling following initial ALK-TKI treatment.

Several studies have reported that the *EML4-ALK* variant influences the benefit of ALK inhibitors [57]. Specifically, patients with *EML4-ALK* V3 have been found to be more prone to developing resistance mutations (particularly ALK G1202R) and have lower median progression-free survival compared to V1 when treated with second-generation ALK inhibitors [58-60]. In our cohort, we found that patients with V1/V2 who had HER3 overexpression in primary or secondary tumors showed significantly shorter OS compared to those without HER3 overexpression. However, in the V3 group, HER3 overexpression did not correlate with a poor outcome in primary tumors. In the context of responsiveness to ALK inhibitors, the V3 group, known for its high kinase activity, structural stability and reduced sensitivity, may experience a lesser impact on prognosis from HER3 overexpression. Conversely, in the V1/V2 group, which is generally more sensitive to ALK inhibitors, HER3 overexpression could significantly contribute to oncogenic signaling, influencing rebound kinetics in response to ALK-TKI therapy and affecting treatment outcomes [61].

Our in vitro data revealed that HRG1 induced PI3K/AKT signaling activation and phosphorylation of ALK in ALK-positive NSCLC cell lines and a notable reduction of RTK expression

when lorlatinib was combined with erlotinib. These indicate that the combined use of ALK- and EGFR-inhibitors could be an effective strategy to overcome HER3 overexpression in ALK-positive cancers. While several studies demonstrated the effectiveness of combining crizotinib or lorlatinib with an EGFR inhibitor in inhibiting the growth of ALK inhibitor-resistant clones, the specific involvement of HER3 overexpression in this context has yet to be studied [41, 62]. While there is a need to explore the physiological roles of HRG1 expression in ALK-TKI resistant lung cancers further, the combination of a HER3-targeting antibody with ALK-TKI may be an efficient treatment strategy.

We highlighted HER3 overexpression as a potential resistance mechanism, particularly observed in *EML4-ALK* V1/V2 variants. However, our study had limitations, such as a restricted number of cases and an uneven distribution of mutation types among patient groups. These factors impacted our ability to perform detailed subgroup analyses, including survival assessments. As an unavoidable feature of this retrospective analysis, another limitation arises from the inclusion of patients who received ALK-TKIs at various time points throughout their disease course. This implies that the OS data could be confounded by the frequency and duration of post-progression treatments, including treatment crossover in the crizotinib arm, potentially limiting the OS results.

5. Conclusion

Our study investigated the expression of the ERBB family and c-MET in primary and secondary tumors of patients with *ALK*-positive NSCLC. We observed that HER3 overexpression commonly occurred in ALK-TKI naïve tumors and could serve as a potential prognostic marker of a poor outcome in primary tumors. Furthermore, HER3 overexpression was identified as a predictor of adverse outcomes in a specific subgroup of patients with *EML4-ALK* V1/V2. These findings indicate that evaluating HER3 expression status can be crucial for achieving improved clinical outcomes in *ALK*-positive NSCLC treated with ALK inhibitors.

Chapter 3: Profile of tumor microenvironment in PD-L1-positive and PD-L1-negative *ALK*-positive non-small cell lung cancer

1. Introduction

Immune checkpoint inhibitors (ICIs) targeting programmed cell death-1 (PD-1), programmed cell death ligand-1 (PD-L1), and CTLA-4 have significantly advanced the disease control of non-small cell lung cancer (NSCLC). Previous trials have reported that the maximum response rate to ICIs is typically around 20%, with an overall survival (OS) benefit observed in unselected NSCLC patients [63, 64]. However, these therapies have been less effective in patients harboring oncogenic driver mutations, such as those involving *EGFR* or *ALK* [65]. To date, it remains unclear why patients with ALK-positive NSCLC do not benefit from ICIs.

Previous studies have shown that PD-L1 expression is associated with *ALK* fusion genes in NSCLC cell lines, and that overexpression of the *ALK* fusion protein can increase PD-L1 expression [66]. The *EML4-ALK* fusion is hypothesized to create an immunosuppressive tumor microenvironment (TME) by activating downstream oncogenic signaling pathways, including the PI3K, MAPK, and Hippo pathways (Fig. 1) [66-68].

Preclinical and clinical studies have demonstrated an upregulation of immune checkpoints such as PD-L1 in de novo *ALK*-positive tumors, raising questions about whether ICIs alone or in combination with targeted TKIs would offer clinical benefits in *ALK*-positive NSCLC. Retrospective studies from a global multicenter network and a U.S. national oncology database have shown that patients with *ALK*-positive NSCLC tumors are relatively resistant to single-agent ICI therapy, with a median progression-free survival of about 2-3 months [69, 70]. The upregulation of PD-L1 expression in *ALK*-positive NSCLC, as shown in preclinical models, has not translated into an improved clinical benefit with ICI. This may be due to multiple factors, including a TME characterized by a lack of infiltrating CD8+ T cells and a complex interplay of constituents such as PD-L1 expressing tumor-associated macrophages (TAMs) and induced FOXP3+ regulatory T cells. Furthermore, *ALK*-positive NSCLC presents with fewer non-synonymous mutations compared to smoking-associated NSCLC, resulting in a less inflamed TME as well as reduced neoantigen generation, leading to a potentially weaker response to ICI [71].

In this study, we aim to investigate PD-L1 expression in *ALK*-positive NSCLC patients and analyze the relationship and clarify its impact on the outcome of ALK-TKI therapy. We explore the TME using immunohistochemical staining of CD3, CD4, CD8, PD-1, and FOXP3 to elucidate the mechanisms affecting the relationship between PD-L1 expression and the outcome of ALK-TKI. Additionally, we compare the spatial profiles of gene expression in PD-L1-negative and PD-L1-positive

samples to investigate the immune biology of *ALK*-positive NSCLC.

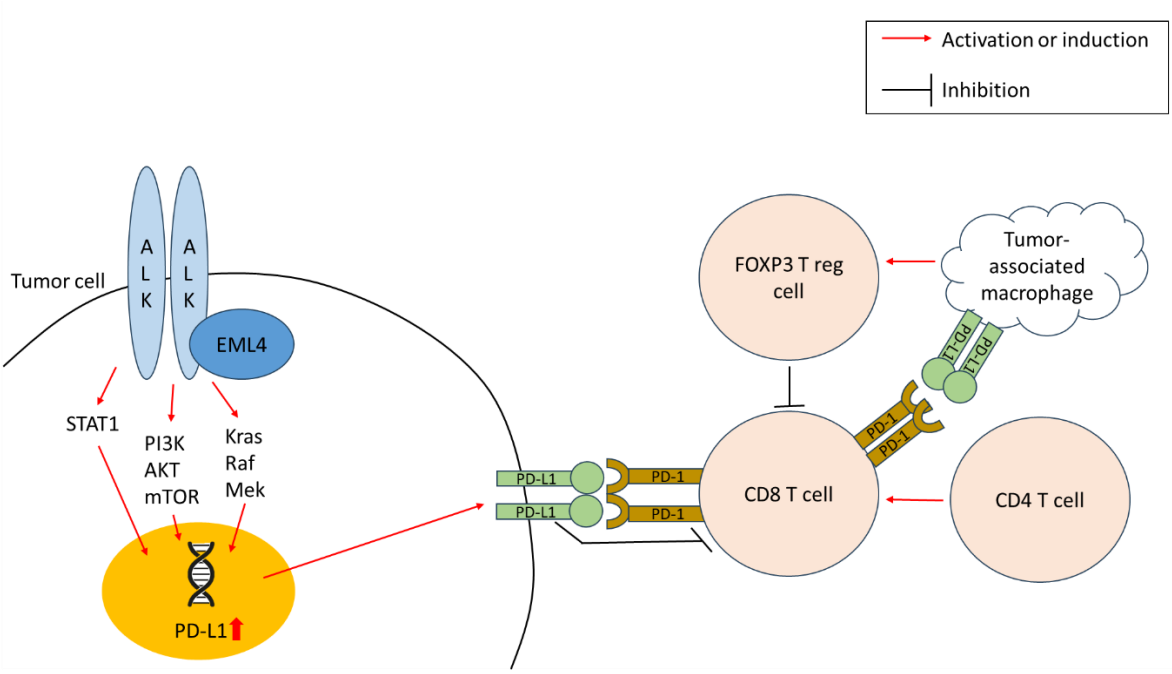

Fig. 1. Tumor microenvironment in ALK-positive non-small cell lung cancer with the PD-1/PD-L1 pathway in tumor cells, tumor-associated macrophages (TAMs), and T cells. PD-L1 expression in tumor cells is upregulated by activation of (1) JAK/STAT pathway; (2) PI3K/Akt pathway; (3) MEK/ERK pathway. PD-L1 on tumor cells and/or TAMs interact with PD-1 on T cells, leading to inhibition of T cell receptor signaling pathway and subsequent T cell exhaustion.

2. Materials and methods

2.1. Study cohort

We retrospectively collected data from patients with *ALK*-positive, advanced-stage NSCLC (stage III or IV) who were treated with ALK-TKI at Asan Medical Center between 2011 and 2021. All cases were pathologically confirmed as *ALK*-positive NSCLC by ALK D5F3 immunohistochemistry, *ALK* fluorescent in situ hybridization (FISH) analysis using a break-apart probe specific for the *ALK* locus (Vysis LSI ALK dual-color, break-apart rearrangement probe; Abbott Molecular, IL, USA), or clinically targeted next-generation sequencing (NGS) using the MiSeq platform (Illumina) with OncoPanel AMC version 3.

2.2. Tissue specimens and immunohistochemistry

Immunohistochemistry (IHC) staining was performed on available formalin-fixed, paraffin-embedded (FFPE) tissues which were primary tumors obtained at initial diagnosis. Whole slides of 5 μm thick tissue sections were stained for PD-L1 using the 22C3 pharmDx Kit (Agilent Technologies, Santa Clara, CA, USA) on the Dako Autostainer Link 48 platform and SP263 (Ventana Medical Systems, Tucson,

AZ, USA), following the manufacturers' instructions. IHC staining for CD3 (Polyclonal, 1:100, Agilent), CD4 (SP35, 1:16, Ventana Medical Systems), CD8 (C8/144B, 1:400, Cell Marque, Rocklin, CA), FOXP3 (236A/E7, 1:100, Abcam, Cambridge, United Kingdom), and PD-1 (MRQ-22, 1:1000, Cell Marque) was performed on whole slides using a fully automated assay on the Ventana BenchMark XT Autostainer (Ventana Medical Systems, Tucson, AZ).

PD-L1 immunoscoring was based on the tumor proportion score (TPS). Both the 22C3 and SP263 assays were assessed semi-quantitatively and reported as TPS, which is calculated by dividing the number of stained tumor cells by the total number of viable tumor cells. Clinically relevant thresholds of 1% and 50% were established, and the results in this study were categorized into two groups: < 1% (negative) and ≥ 1% (positive). For survival analysis, the positive group was subclassified into a low expression group (≥ 1% and < 50% for 22C3, ≥ 1% and < 10% for SP263) and a high expression group (≥ 50% for 22C3, ≥ 10% for SP263), respectively.

For quantifying the tumor immune cell population, the densities of CD3, CD4, CD8, PD-1, and FOXP3 positive cells in digital whole slide images were measured using QuPath V.0.5.1. All stained slides were scanned with a whole-slide scanner (NanoZoomer-SQ, Hamamatsu Photonics K.K., Hamamatsu, Japan). Positive cells in the tumor areas were counted using the Positive Cell Detection module in QuPath and the cut-off values for each immunostaining were adjusted. Positive cell densities in the tumor area were measured as the number of positive cells per mm² of tumor area (cell counts/mm²).

2.3. Spatial transcriptomic analysis

Two samples, one with PD-L1 positive ALK positive NSCLC and one with PD-L1 negative ALK positive NSCLC, were analyzed for spatial sequencing. To assess the quality of FFPE tissue blocks, RNA was extracted from 5 μm-thick FFPE sections according to the manufacturer’s recommendation. Libraries were prepared according to the Visium Cytassist workflow. The Space Ranger software (version 1.3.1) from 10x Genomics was used for sample demultiplexing, alignment, tissue and fiducial detection, and UMI counting. Data were analyzed and visualized using the 10x Genomics Loupe Browser. Differential gene expression analysis was performed with Seurat's ‘FindAllMarkers’ function. Cluster-specific spots underwent differentially expressed genes (DEGs) analysis against other clusters for each sample. The ‘Aggr’ function was used for merged tSNE analysis to identify common cell populations. Log fold change and adjusted p-values were obtained for all genes. For cell type annotation, the CIBERSORTx algorithm was used for the immune cell analysis [72]. Additionally, We used markers for T cell activation or inhibition, antigen presentation, phagocytosis as described [73]. T cell (CD3D, CD3E, CD3G, TRAC), B cell (CD79A, IGHM, IGHG3, MS4A1), NK cell (KLRF1, GNLY, CD247, KLRG1), fibroblast (DCN, THY1, COL1A1, COL1A2), endothelial cell (PECAM1, CLDN5, FLT1, RAMP2), dendritic cell (CLEC9A, CD1C), neutrophil (S100A8, S100A9), macrophage (CD68, CD163), cytotoxic T cell (CD8A), and Treg

cell (FOXP3) were also used [74, 75].

2.4. Statistical analysis

The expression levels of PD-L1, CD3, CD4, CD8, and FOXP3 according to PD-1 expression or disease progression status were compared using Student's t-test. The 5-year progression-free survival (PFS) was determined using Kaplan-Meier analysis, with survival differences evaluated by the log-rank test. PFS was calculated from the initiation of ALK-TKI treatment to the date of disease progression or death from any cause, and was censored at the last visit for patients alive without documented disease progression. Statistical analyses were conducted using SPSS version 21.0.0 and R version 4.2.1, considering a P-value < 0.05 as significant.

3. Results

3.1. Comparison of PD-L1 expression levels and their impact on the effect of ALK-TKI treatment outcomes

Of the 69 primary tumor specimens, 68 were assessable for PD-L1 expression and the remaining one case was inadequate due to insufficient tumor cells. For the 68 primary tumor specimens assessed, 19 cases (28%) were PD-L1 positive with the 22C3 assay, and 23 cases (34%) were PD-L1 positive with the SP263 assay. The median duration of follow-up was 13 months (range, 0 – 60) and the median 5-year PFS was 15 months (95% CI, 12.16 – 17.84). Among patients treated with ALK-TKI, PD-L1 status did not significantly influence their PFS. However, cases with high PD-L1 expression (22C3 ≥ 50% or SP263 ≥ 10%) exhibited a trend toward longer survival (P = 0.297 and 0.186, respectively; Fig. 2a and 2b). On a continuous level of PD-L1 expression, patients in the disease progression group showed significantly lower 22C3 expression than those without progression (P = 0.034; Fig. 2c). For SP263, the difference was not significant, although the progression group tended to have lower expression levels (P = 0.717; Fig. 2d).

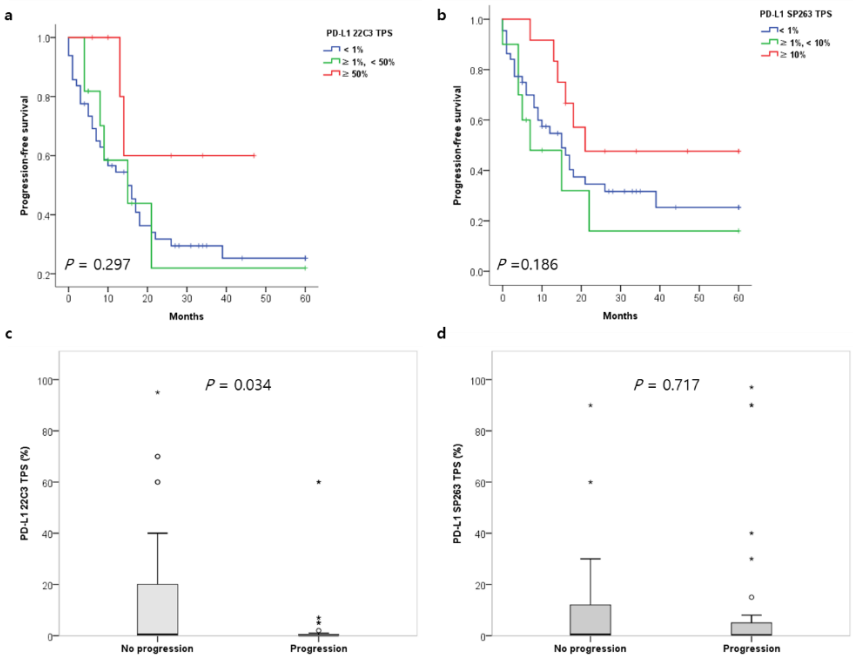

Fig. 2. Association of PD-L1 expression with disease progression. Analysis of progression-free survival using 22C3 assay (a) and SP263 assay (b). Comparative PD-L1 expression levels between patients with progression and those without progression (c – d).

3.2. Immune cell densities and PD-L1 expression

Of the 68 cases analyzed for PD-L1 expression, 20 were additionally analyzed for tumor immune cell densities of CD3, CD4, CD8, FOXP3, and PD-1-positive T cells. These cases were surgical resection specimens available for further tumor immune cell densities IHC analysis. Intratumoral immune cell densities of each marker showed significant positive correlations with each other (data not shown). Overall, immune cell densities were not significantly different between the PD-L1-positive and negative group in 22C3 (Fig. 3a–3e) and SP263 assays (Fig. 3i–3m). However, the densities of PD-1 and PD-1/CD8 showed a higher tendency in the PD-L1 positive group compared to the PD-L1 negative group in both assays.

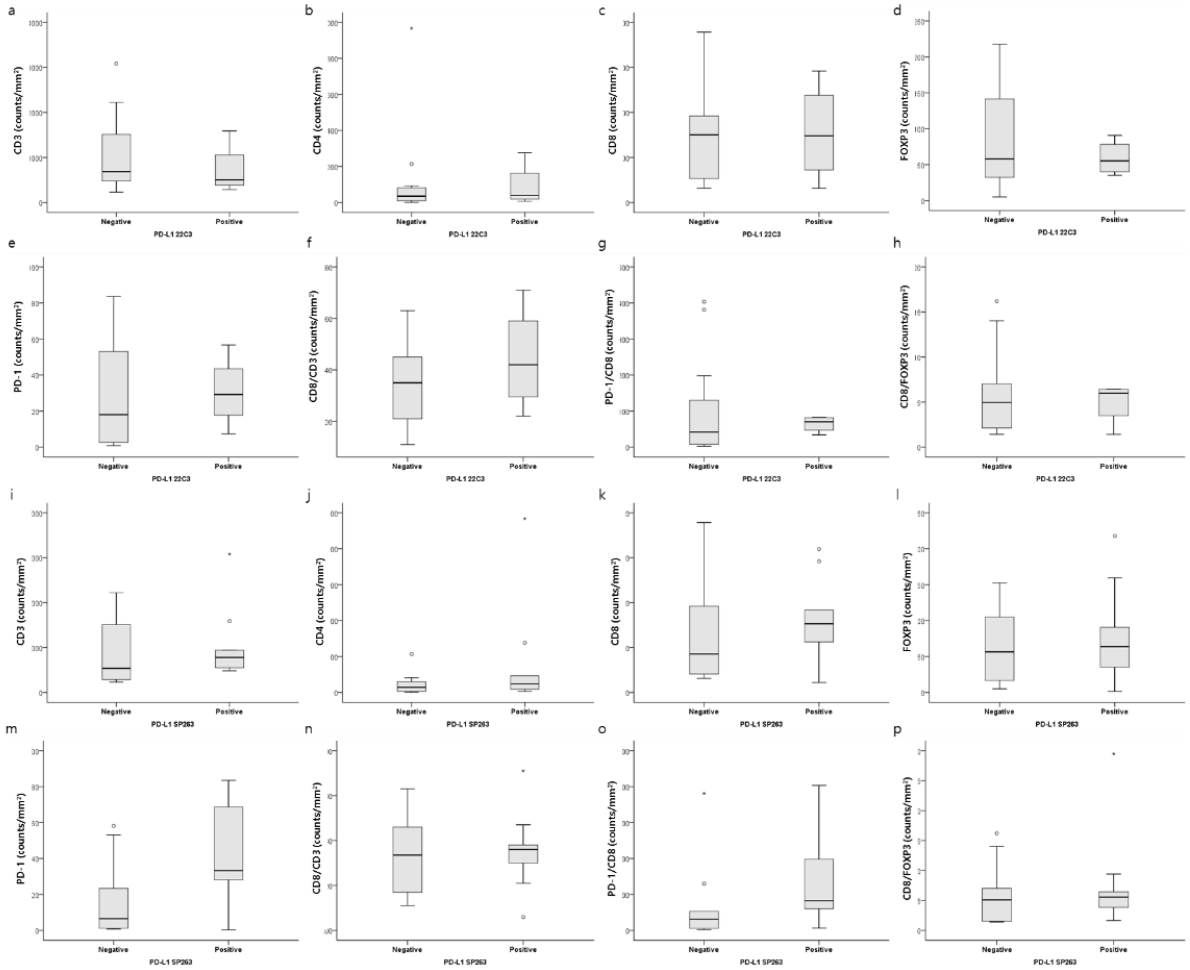

Fig. 3. Immune cell densities and PD-L1 expression. Densities of positive cells for CD3, CD4, CD8, FOXP3, and PD-1 immunohistochemical staining between PD-L1 positive and negative cases (a–h, 22C3; i–p, SP263).

3.3. Comparison of immune cell-related gene expression and distribution in PD-L1 positive and negative cases

Using markers for immune cell-related genes, the median normalized average gene expression counts were compared. *CD274* (encoding PD-L1) expression was higher in the PD-L1 positive case, while *PDCD1* (encoding PD-1) levels were not significantly different (Fig. 4a). *CD68,* related to pan-macrophages, and *CD163,* related to M2-like macrophages, were predominant in both cases but were relatively higher in the PD-L1 positive case (Fig. 4b). In the distribution of immune cell populations using CIBERSORTx, macrophages were predominant, with M2 macrophages being the major type and slightly higher in the PD-L1 positive case (Fig. 4c). Expression levels of genes related to T cell activation and inhibition were higher in PD-L1 positive case (Fig. 5a). For TME components analysis, T cell, B cell, and NK cell-related genes were highly expressed in PD-L1 negative cases, while macrophage-related

genes were predominant and slightly higher in PD-L1 positive cases (Fig. 5b). In the t-SNE plot, coexpression spots of *CD274* and *PDCD1* were rare: 52/4746 (1%) spots in the PD-L1 negative case and 230/4817 (5%) spots in the PD-L1 positive case (Fig. 6a and 6b). Among the coexpression spots, *CD68* and *CD163* showed prevalent expression levels compared to other immune-related genes (Fig. 6c). Moreover, in spots expressing *CD163* or *CD8*, PDCD1 expression levels were slightly higher in PD-L1 positive cases compared to the notable difference in *CD274* levels (Fig. 6d).

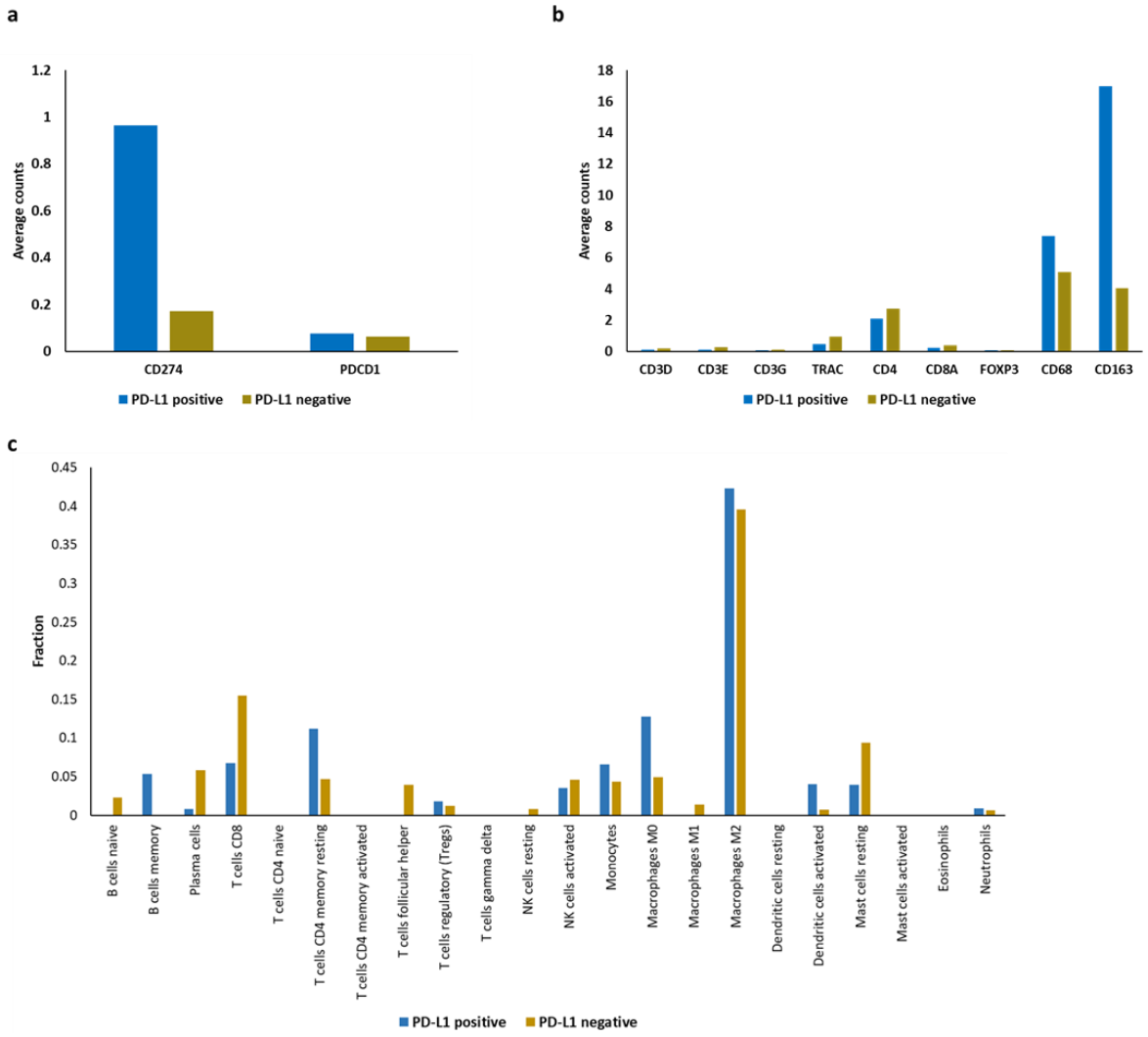

Fig. 4. Comparison of CD274, PDCD1, and tumor microenvironment composition in PD-L1 positive and negative cases. Comparison of *CD274* and *PDCD1* expression levels (a), tumor microenvironment composition using cell type markers (b), and immune cell population distribution using CIBERSORTx analyses (c).

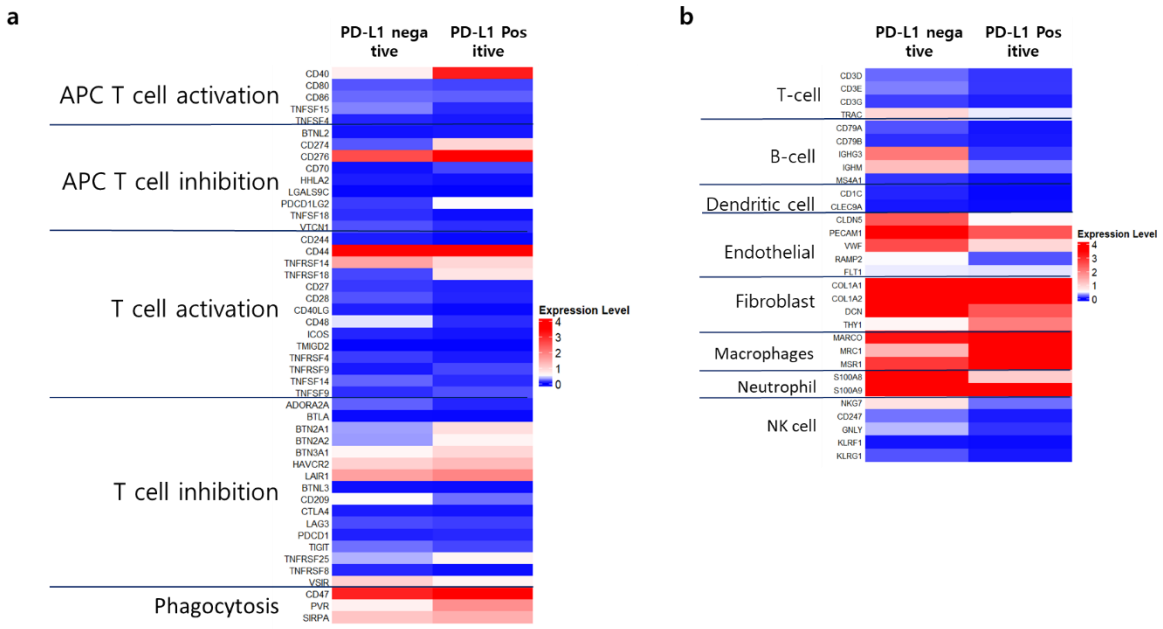

Fig. 5. Heatmap of gene expression in the tumor microenvironment. Expression of regulatory genes for T cell activation and inhibition (a) and components involving the tumor microenvironment (b).

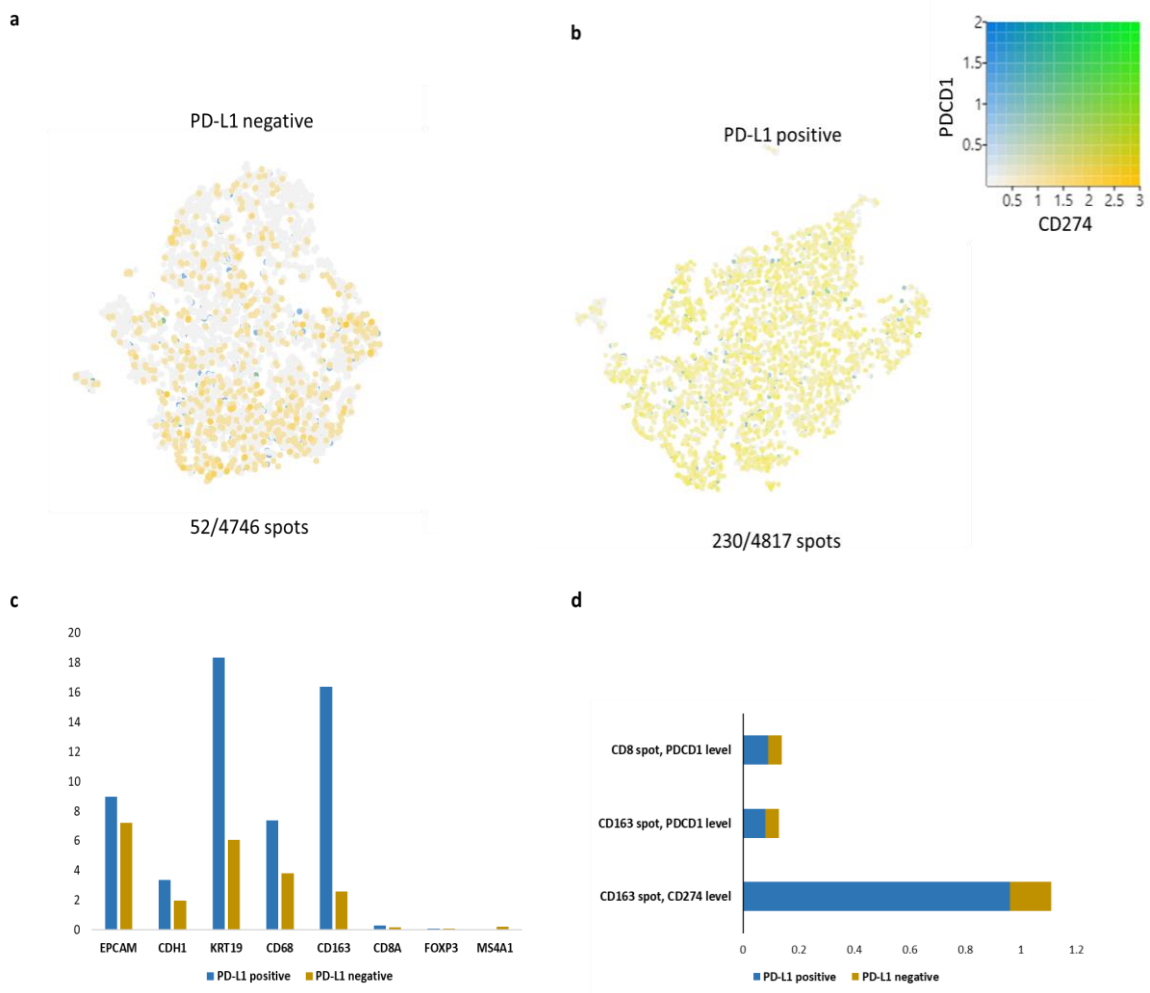

Fig. 6. Coexpression and immune cell-related gene expression in PD-L1 positive and negative cases. Coexpression of *CD274* and *PDCD1* in PD-L1 positive and negative cases shown by t-SNE (a, b) and comparison of immune cell-related gene expression profiles (c). Expression levels of *CD274* or *PDCD1* within the CD8, CD163, or CD68 expression spots, respectively (d).

4. Discussion

In this study, we explored the relationship between PD-L1 expression and prognosis in *ALK*-positive NSCLC, and investigated whether this relationship is associated with T cell density or immune-related gene expression profiles using IHC and spatial transcriptomics. High PD-L1 expression showed a trend toward longer PFS and was less associated with disease progression. Although T-cell densities on IHC did not differ between PD-L1 positive and negative cases, spatial transcriptomic analysis uncovered differential expression patterns of immune cell-related genes between PD-L1 positive and negative cases. This finding also highlights the significant role of macrophages, especially M2 macrophages, in the context of high PD-L1 expression.

The prognostic role of PD-L1 expression in *ALK*-positive NSCLC patients has not been clearly defined, and prior studies have shown conflicting results regarding its association with outcomes in these patients. We observed that high PD-L1 expression in *ALK*-positive NSCLC tended to be associated with longer PFS, although the differences were not statistically significant (P = 0.297 in 22C3 and P = 0.186 in SP263). Conversely, lower PD-L1 expression was significantly associated with disease progression in the 22C3 assay (P = 0.034). However, these findings conflict with prior studies on non-driver mutant NSCLC tumors, which have shown that high PD-L1 expression induces immune escape, leading to poor outcomes [76-78]. This discrepancy suggests that the known mechanism of PD-L1's immunosuppressive action in non-driver mutant NSCLC may differ in *ALK*-positive NSCLC.

Several studies have documented a correlation between PD-L1 expression and the density of CD8+ T cells in lung cancer [79, 80]. CD8, primarily found on cytotoxic T cells, is essential for the cellular immune system and plays a vital role in cell-mediated antitumor immune responses. Since CD8+ T cells induce PD-L1 expression in tumor cells through the production of interferon gamma, earlier studies have highlighted the link between CD8+ T cells and PD-L1 expression in NSCLC, along with the prognostic significance of PD-L1 expression combined with CD8+ T cell density [81]. Nevertheless, in our current study, we did not observe a significant association between PD-L1 expression and tumor infiltrating lymphocytes (TIL) densities, including CD8+ T cells, in ALK-positive NSCLC. Unlike non-driver mutant NSCLC, ALK-positive NSCLC generally has fewer TILs, including CD8+ T cells. Consequently, the distribution of TILs may not exhibit a significant difference based on PD-L1 expression status in ALK-positive NSCLC [71].

Although the assessment of TILs in IHC studies could not explain the conflicting results between PD-L1 expression and prognosis in *ALK*-positive lung cancer, spatial transcriptomic analysis revealed minimal coexpression of *CD274* and *PDCD1* in the PD-L1 positive case, with only 230 out of 4817 spots showing coexpression. Moreover, the PD-L1 positive case showed the low expression of *PDCD1* in macrophages and CD8+ T cells, despite the high expression of *CD274.* This rarity of coexpression suggests that *ALK*-positive NSCLC may not be characterized by direct contact between PD-1 receptor-bearing cells and PD-L1 ligand-expressing cells, which could be a potential reason for the limited efficacy of ICIs in this subgroup of NSCLC. Furthermore, within the coexpression spots of *CD274* and *PDCD1, CD163* was the most highly expressed immune cell-related genes. Thus, in PD-L1 positive *ALK*-positive NSCLC, the role of PD-L1 expressing TAMs may be more significant compared to the commonly known interaction mechanism of PD-1 expressing CD8+ T cells.

The spatial profile in our study is similar to that observed in triple-negative breast cancer (TNBC), which has shown limited effects of ICI compared to other subtypes of breast cancer. A prior study showed higher levels of PD-L1 positive TAMs but relatively lower levels of PD-1 positive immune cells in PD-L1 positive TNBCs, suggesting that these findings may not lead to immune escape, which

might contribute to the limited effect of ICI in TNBC. [74]. Similarly, the retained immune response in PD-L1 positive *ALK*-positive NSCLC might contribute to the controversial relationship between PD-L1 expression and prognosis. In *ALK*-positive NSCLC, our findings suggest that immune suppression may not primarily occur through the interaction between PD-L1 expressing tumor cells and PD-1 expressing CD8+ T cells, as previously understood. Instead, a different mechanism involving TAMs might play a more significant role. This shift in perspective highlights the importance of investigating the role of TAMs in PD-L1 expression within *ALK*-positive NSCLC. Future research should focus on this alternative mechanism to better understand and potentially target the unique immune environment in these patients.

Our studies have the limitation of needing comparative analyses involving groups with non-driver mutations or other known driver mutations, such as EGFR and KRAS, to better understand the unique immune landscapes of *ALK*-positive NSCLC. Additionally, validation at the protein level, including CD68 and CD163 markers with coexpression of PD-L1 or PD-1 using multiplex immunoassays, is essential to corroborate our transcriptomic results and elucidate the precise mechanisms underlying immune regulation in this context. Although our study was conducted on a limited number of cases, its findings provide valuable insights and suggest a new direction for future research. The significance of this study lies in proposing a different perspective for understanding the immune mechanisms in *ALK*-positive NSCLC, highlighting the potential role of TAMs in PD-L1 expression.

5. Conclusion

In PD-L1 positive *ALK*-positive NSCLC, the role of TAMs appears to be more significant than that of PD-1 expressing CD8+ T cells in the interaction between PD-L1 expressing tumor cells and immune cells. This highlights a potential alternative mechanism of immune regulation in this subtype, warranting further investigation into the role of TAMs.

General conclusion

Biomarkers in advanced cancers offer valuable prognostic insights and therapeutic targets. The NEK9-EG5 axis is essential for microtubule polymerization and centrosome separation, with aberrant expression linked to metastasis and poor prognosis in pT3 colon cancer, highlighting the need for further research into their tissue-specific roles. HER3 overexpression, in *EML4-ALK* V1/V2 variants, enhances oncogenic signaling and serves as a poor prognostic marker in ALK-TKI naïve tumors and indicates a potential resistance mechanism. Combining ALK and EGFR inhibitors may help overcome this resistance. In PD-L1 expressing *ALK*-positive NSCLC, M2 macrophages, which are a major subtype of

TAMs, are significant immune cells in the TME. Our findings offer valuable insights and propose a new research direction, emphasizing the need for further studies to fully understand the unique immune landscape of ALK-positive NSCLC.

References

1. Riihimäki, M., et al., *Patterns of metastasis in colon and rectal cancer.* Scientific reports, 2016. **6**(1): p. 1-9.
2. Rawla, P., T. Sunkara, and A. Barsouk, *Epidemiology of colorectal cancer: incidence, mortality, survival, and risk factors.* Gastroenterology Review/Przegląd Gastroenterologiczny, 2019. **14**(2): p. 89-103.
3. Ries, L., D. Melbert, and M. Krapcho, *SEER cancer statistics review 1975–2012.* Bethesda, MD: NCI, 2014.
4. Fry, A.M., et al., *Cell cycle regulation by the NEK family of protein kinases.* Journal of cell science, 2012. **125**(19): p. 4423-4433.
5. Yissachar, N., et al., *Nek7 kinase is enriched at the centrosome, and is required for proper spindle assembly and mitotic progression.* FEBS letters, 2006. **580**(27): p. 6489-6495.
6. Neal, C.P., et al., *Overexpression of the Nek2 kinase in colorectal cancer correlates with beta-catenin relocalization and shortened cancer-specific survival.* Journal of surgical oncology, 2014. **110**(7): p. 828-838.
7. Kasap, E., et al., *The potential role of the NEK6, AURKA, AURKB, and PAK1 genes in adenomatous colorectal polyps and colorectal adenocarcinoma.* Tumor Biology, 2016. **37**(3): p. 3071-3080.
8. Xu, Z., et al., *Decreased Nek9 expression correlates with aggressive behaviour and predicts unfavourable prognosis in breast cancer.* Pathology, 2020. **52**(3): p. 329-335.
9. Kapitein, L.C., et al., *The bipolar mitotic kinesin Eg5 moves on both microtubules that it crosslinks.* Nature, 2005. **435**(7038): p. 114-118.
10. Nekooki-Machida, Y. and H. Hagiwara, *Role of tubulin acetylation in cellular functions and diseases.* Medical molecular morphology, 2020. **53**(4): p. 191-197.
11. O'Regan, L., et al., *EML4–ALK V3 oncogenic fusion proteins promote microtubule stabilization and accelerated migration through NEK9 and NEK7.* Journal of cell science, 2020. **133**(9): p. jcs241505.
12. Cao, H., et al., *Epithelial–mesenchymal transition in colorectal cancer metastasis: a system review.* Pathology-Research and Practice, 2015. **211**(8): p. 557-569.
13. Pavlič, A., et al., *Epithelial-mesenchymal transition in colorectal carcinoma: Comparison between primary tumor, lymph node and liver metastases.* Frontiers in Oncology, 2021: p. 1504.

14. Paul, C.D., P. Mistriotis, and K. Konstantopoulos, *Cancer cell motility: lessons from migration in confined spaces.* Nature reviews cancer, 2017. **17**(2): p. 131-140.
15. Lennartz, M., et al., *Large-scale tissue microarray evaluation corroborates high specificity of high-level arginase-1 immunostaining for hepatocellular carcinoma.* Diagnostics, 2021. **11**(12): p. 2351.
16. Saijo, T., et al., *Eg5 expression is closely correlated with the response of advanced non-small cell lung cancer to antimitotic agents combined with platinum chemotherapy.* Lung Cancer, 2006. **54**(2): p. 217-225.
17. Higashi, Y., et al., *Loss of claudin-1 expression correlates with malignancy of hepatocellular carcinoma.* Journal of Surgical Research, 2007. **139**(1): p. 68-76.
18. Pino, M.S., et al., *Epithelial to mesenchymal transition is impaired in colon cancer cells with microsatellite instability.* Gastroenterology, 2010. **138**(4): p. 1406-1417.
19. Al-Maghrabi, J., *Vimentin immunoexpression is associated with higher tumor grade, metastasis, and shorter survival in colorectal cancer.* International Journal of Clinical and Experimental Pathology, 2020. **13**(3): p. 493.
20. Gao, Z.-H., et al., *Differential β-catenin expression levels are associated with morphological features and prognosis of colorectal cancer.* Oncology letters, 2014. **8**(5): p. 2069-2076.
21. Jin, P., S. Hardy, and D.O. Morgan, *Nuclear localization of cyclin B1 controls mitotic entry after DNA damage.* The Journal of cell biology, 1998. **141**(4): p. 875-885.
22. Kandel, E.S., et al., *Activation of Akt/protein kinase B overcomes a G2/M cell cycle checkpoint induced by DNA damage.* Molecular and cellular biology, 2002. **22**(22): p. 7831-7841.
23. Kurioka, D., et al., *NEK9-dependent proliferation of cancer cells lacking functional p53.* Scientific reports, 2014. **4**(1): p. 1-8.
24. Lu, G., et al., *NEK9, a novel effector of IL-6/STAT3, regulates metastasis of gastric cancer by targeting ARHGEF2 phosphorylation.* Theranostics, 2021. **11**(5): p. 2460.
25. Janke, C. and G. Montagnac, *Causes and consequences of microtubule acetylation.* Current Biology, 2017. **27**(23): p. R1287-R1292.
26. Bertran, M.T., et al., *Nek9 is a Plk1-activated kinase that controls early centrosome separation through Nek6/7 and Eg5.* The EMBO journal, 2011. **30**(13): p. 2634-2647.
27. Rapley, J., et al., *The NIMA-family kinase Nek6 phosphorylates the kinesin Eg5 at a novel site necessary for mitotic spindle formation.* Journal of cell science, 2008. **121**(23): p. 3912-3921.
28. Eibes, S., et al., *Nek9 phosphorylation defines a new role for TPX2 in Eg5-dependent centrosome separation before nuclear envelope breakdown.* Current Biology, 2018. **28**(1): p. 121-129. e4.
29. Boggs, A.E., et al., *α-Tubulin acetylation elevated in metastatic and basal-like breast cancer cells promotes microtentacle formation, adhesion, and invasive migration.* Cancer research,

2015. **75**(1): p. 203-215.

30. Cavazza, T., P. Malgaretti, and I. Vernos, *The sequential activation of the mitotic microtubule assembly pathways favors bipolar spindle formation.* Molecular biology of the cell, 2016. **27**(19): p. 2935-2945.
31. Wickström, S.A., et al., *CYLD negatively regulates cell-cycle progression by inactivating HDAC6 and increasing the levels of acetylated tubulin.* The EMBO Journal, 2010. **29**(1): p. 131-144.
32. Soda, M., et al., *Identification of the transforming EML4–ALK fusion gene in non-small-cell lung cancer.* Nature, 2007. **448**(7153): p. 561-566.
33. Ducray, S.P., et al., *The Transcriptional Roles of ALK Fusion Proteins in Tumorigenesis.* Cancers (Basel), 2019. **11**(8).
34. Sabir, S.R., et al., *EML4-ALK variants: biological and molecular properties, and the implications for patients.* Cancers, 2017. **9**(9): p. 118.
35. Koivunen, J.P., et al., *EML4-ALK fusion gene and efficacy of an ALK kinase inhibitor in lung cancer.* Clin Cancer Res, 2008. **14**(13): p. 4275-83.
36. Dong, X., et al., *Elucidation of Resistance Mechanisms to Second-Generation ALK Inhibitors Alectinib and Ceritinib in Non-Small Cell Lung Cancer Cells.* Neoplasia, 2016. **18**(3): p. 162-71.
37. Cooper, A.J., L.V. Sequist, and J.J. Lin, *Third-generation EGFR and ALK inhibitors: mechanisms of resistance and management.* Nat Rev Clin Oncol, 2022. **19**(8): p. 499-514.
38. Smolle, E., et al., *Current Knowledge about Mechanisms of Drug Resistance against ALK Inhibitors in Non-Small Cell Lung Cancer.* Cancers (Basel), 2021. **13**(4).
39. Isozaki, H., et al., *Non-Small Cell Lung Cancer Cells Acquire Resistance to the ALK Inhibitor Alectinib by Activating Alternative Receptor Tyrosine Kinases.* Cancer Res, 2016. **76**(6): p. 1506-16.
40. Dagogo-Jack, I., et al., *MET Alterations Are a Recurring and Actionable Resistance Mechanism in ALK-Positive Lung CancerMET Alterations in ALK-Positive Lung Cancer.* Clinical Cancer Research, 2020. **26**(11): p. 2535-2545.
41. Katayama, Y., et al., *Adaptive resistance to lorlatinib via EGFR signaling in ALK-rearranged lung cancer.* NPJ Precis Oncol, 2023. **7**(1): p. 12.
42. Ying, J., et al., *Diagnostic value of a novel fully automated immunochemistry assay for detection of ALK rearrangement in primary lung adenocarcinoma.* Ann Oncol, 2013. **24**(10): p. 2589-2593.
43. Paik, J.H., et al., *Screening of anaplastic lymphoma kinase rearrangement by immunohistochemistry in non-small cell lung cancer: correlation with fluorescence in situ hybridization.* J Thorac Oncol, 2011. **6**(3): p. 466-72.
44. Hwang, H.S., D. Kim, and J. Choi, *Distinct mutational profile and immune microenvironment in microsatellite-unstable and POLE-mutated tumors.* J Immunother Cancer, 2021. **9**(10).

45. Kim, J.H., et al., *Real-world utility of next-generation sequencing for targeted gene analysis and its application to treatment in lung adenocarcinoma.* Cancer Med, 2021. **10**(10): p. 3197-3204.
46. Koh, Y.W., et al., *Receptor tyrosine kinases MET and RON as prognostic factors in diffuse large B-cell lymphoma patients receiving R-CHOP.* Cancer Sci, 2013. **104**(9): p. 1245-51.
47. Li, A.R., et al., *EGFR mutations in lung adenocarcinomas: clinical testing experience and relationship to EGFR gene copy number and immunohistochemical expression.* The Journal of Molecular Diagnostics, 2008. **10**(3): p. 242-248.
48. Tsuta, K., et al., *c-MET/phospho-MET protein expression and MET gene copy number in non-small cell lung carcinomas.* Journal of thoracic oncology, 2012. **7**(2): p. 331-339.
49. Cox, G., et al., *Herceptest: Her2 expression and gene amplification in non-small cell lung cancer.* International journal of cancer, 2001. **92**(4): p. 480-483.
50. Rüschoff, J., et al., *HER2 testing in gastric cancer: a practical approach.* Modern Pathology, 2012. **25**(5): p. 637-650.
51. Koeppen, H., et al., *Overexpression of HER2/neu in solid tumours: an immunohistochemical survey.* Histopathology, 2001. **38**(2): p. 96-104.
52. Christopoulos, P., et al., *EML4-ALK V3, treatment resistance, and survival: refining the diagnosis of ALK(+) NSCLC.* J Thorac Dis, 2018. **10**(Suppl 17): p. S1989-s1991.
53. Tanizaki, J., et al., *Activation of HER family signaling as a mechanism of acquired resistance to ALK inhibitors in EML4-ALK-positive non-small cell lung cancer.* Clin Cancer Res, 2012. **18**(22): p. 6219-26.
54. Tanimura, K., et al., *HER3 activation contributes toward the emergence of ALK inhibitor-tolerant cells in ALK-rearranged lung cancer with mesenchymal features.* npj Precision Oncology, 2022. **6**(1): p. 5.
55. Wilson, F.H., et al., *A functional landscape of resistance to ALK inhibition in lung cancer.* Cancer Cell, 2015. **27**(3): p. 397-408.
56. Hegde, G.V., et al., *Blocking NRG1 and other ligand-mediated Her4 signaling enhances the magnitude and duration of the chemotherapeutic response of non-small cell lung cancer.* Sci Transl Med, 2013. **5**(171): p. 171ra18.
57. Elshatlawy, M., et al., *EML4-ALK biology and drug resistance in non-small cell lung cancer: a new phase of discoveries.* Molecular Oncology, 2023. **17**(6): p. 950-963.
58. Woo, C.G., et al., *Differential protein stability and clinical responses of EML4-ALK fusion variants to various ALK inhibitors in advanced ALK-rearranged non-small cell lung cancer.* Ann Oncol, 2017. **28**(4): p. 791-797.
59. Tao, H., et al., *Distribution of EML4-ALK fusion variants and clinical outcomes in patients with resected non-small cell lung cancer.* Lung Cancer, 2020. **149**: p. 154-161.
60. Lin, J.J., et al., *Impact of EML4-ALK Variant on Resistance Mechanisms and Clinical Outcomes*

in ALK-Positive Lung Cancer. J Clin Oncol, 2018. **36**(12): p. 1199-1206.

61. Bearz, A., et al., *Efficacy of Lorlatinib in Treatment-Naive Patients With ALK-Positive Advanced NSCLC in Relation to EML4::ALK Variant Type and ALK With or Without TP53 Mutations.* Journal of Thoracic Oncology, 2023. **18**(11): p. 1581-1593.
62. Yamaguchi, N., et al., *Dual ALK and EGFR inhibition targets a mechanism of acquired resistance to the tyrosine kinase inhibitor crizotinib in ALK rearranged lung cancer.* Lung Cancer, 2014. **83**(1): p. 37-43.
63. Brahmer, J., et al., *Nivolumab versus Docetaxel in Advanced Squamous-Cell Non-Small-Cell Lung Cancer.* N Engl J Med, 2015. **373**(2): p. 123-35.
64. Herbst, R.S., et al., *Pembrolizumab versus docetaxel for previously treated, PD-L1-positive, advanced non-small-cell lung cancer (KEYNOTE-010): a randomised controlled trial.* Lancet, 2016. **387**(10027): p. 1540-1550.
65. Gainor, J.F., et al., *EGFR Mutations and ALK Rearrangements Are Associated with Low Response Rates to PD-1 Pathway Blockade in Non-Small Cell Lung Cancer: A Retrospective Analysis.* Clin Cancer Res, 2016. **22**(18): p. 4585-93.
66. Hong, S., et al., *Upregulation of PD-L1 by EML4-ALK fusion protein mediates the immune escape in ALK positive NSCLC: Implication for optional anti-PD-1/PD-L1 immune therapy for ALK-TKIs sensitive and resistant NSCLC patients.* Oncoimmunology, 2016. **5**(3): p. e1094598.
67. Ota, K., et al., *Induction of PD-L1 Expression by the EML4-ALK Oncoprotein and Downstream Signaling Pathways in Non-Small Cell Lung Cancer.* Clin Cancer Res, 2015. **21**(17): p. 4014-21.
68. Nouri, K., et al., *A kinome-wide screen using a NanoLuc LATS luminescent biosensor identifies ALK as a novel regulator of the Hippo pathway in tumorigenesis and immune evasion.* Faseb j, 2019. **33**(11): p. 12487-12499.
69. Jahanzeb, M., et al., *Immunotherapy Treatment Patterns and Outcomes Among ALK-Positive Patients With Non-Small-Cell Lung Cancer.* Clin Lung Cancer, 2021. **22**(1): p. 49-57.
70. Mazieres, J., et al., *Immune checkpoint inhibitors for patients with advanced lung cancer and oncogenic driver alterations: results from the IMMUNOTARGET registry.* Ann Oncol, 2019. **30**(8): p. 1321-1328.
71. Govindan, R., et al., *Genomic landscape of non-small cell lung cancer in smokers and never-smokers.* Cell, 2012. **150**(6): p. 1121-34.
72. Chen, B., et al., *Profiling Tumor Infiltrating Immune Cells with CIBERSORT*, in *Cancer Systems Biology: Methods and Protocols*, L. von Stechow, Editor. 2018, Springer New York: New York, NY. p. 243-259.
73. Zhang, Q., et al., *The spatial transcriptomic landscape of non-small cell lung cancer brain metastasis.* Nat Commun, 2022. **13**(1): p. 5983.

74. Tashireva, L.A., et al., *Spatial Profile of Tumor Microenvironment in PD-L1-Negative and PD-L1-Positive Triple-Negative Breast Cancer.* Int J Mol Sci, 2023. **24**(2).
75. Xie, L., et al., *Spatial transcriptomics reveals heterogeneity of histological subtypes between lepidic and acinar lung adenocarcinoma.* Clin Transl Med, 2024. **14**(2): p. e1573.
76. Du, P., et al., *In vitro and in vivo synergistic efficacy of ceritinib combined with programmed cell death ligand-1 inhibitor in anaplastic lymphoma kinase-rearranged non-small-cell lung cancer.* Cancer Sci, 2020. **111**(6): p. 1887-1898.
77. Chang, G.C., et al., *ALK variants, PD-L1 expression, and their association with outcomes in ALK-positive NSCLC patients.* Sci Rep, 2020. **10**(1): p. 21063.
78. Li, M., et al., *ALK fusion variant 3a/b, concomitant mutations, and high PD-L1 expression were associated with unfavorable clinical response to second-generation ALK TKIs in patients with advanced ALK-rearranged non-small cell lung cancer (GASTO 1061).* Lung Cancer, 2022. **165**: p. 54-62.
79. Konishi, J., et al., *B7-H1 expression on non-small cell lung cancer cells and its relationship with tumor-infiltrating lymphocytes and their PD-1 expression.* Clin Cancer Res, 2004. **10**(15): p. 5094-100.
80. Chen, Y.B., C.Y. Mu, and J.A. Huang, *Clinical significance of programmed death-1 ligand-1 expression in patients with non-small cell lung cancer: a 5-year-follow-up study.* Tumori, 2012. **98**(6): p. 751-5.
81. Tokito, T., et al., *Predictive relevance of PD-L1 expression combined with CD8+ TIL density in stage III non-small cell lung cancer patients receiving concurrent chemoradiotherapy.* Eur J Cancer, 2016. **55**: p. 7-14.

국문요약

연구배경 및 목적

신흥 바이오마커의 탐색은 진행성 암에서 치료 및 맞춤 의학을 발전시키는 데 필수적이다. 본 연구에서는 세 가지 신흥 바이오마커인 대장암에서의 NEK9–EG5 축, *ALK* 양성 비소세포폐암(NSCLC)에서의 HER3, 그리고 *ALK* 양성 NSCLC의 종양 미세환경과 PD-L1 발현의 예후 및 치료적 의미를 조사하였다.

연구재료와 연구방법

대장암 연구를 위해 138명의 pT3 대장암 환자의 조직 샘플에 대해 면역조직화학(IHC) 분석을 수행하여 NEK9, EG5 및 acetyl-α-tubulin 발현을 평가했다. NSCLC 연구에서는 ALK 억제제 노출 전/후 *ALK* 양성 NSCLC조직의 HER3 발현을 평가하기 위해 IHC 염색을 수행하고, HRG1 리간드를 통한 HER3 활성화를 확인하기 위해 western blot 분석을 사용했다. 또한, *ALK* 양성 NSCLC 세포주에서 ALK 및 EGFR 억제제의 병합 치료 효과를 테스트했다. T 세포 아형의 발현 정도를 비교하기 위해 CD3, CD4, CD8, FOXP3, PD-1 IHC 분석, PD-L1 발현 평가를 위해 22C3 및 SP263항체를 사용했다. 또한, 두 개의 대표적인 *ALK* 양성 NSCLC 사례 (각각PD-L1 양성 및 PD-L1 음성)에 대해 spatial transcriptomic analysis를 수행하여 면역세포 관련 유전자 발현 패턴을 분석했다.

연구결과

대장암 환자의 IHC 분석 결과, NEK9 발현은 원격 전이와 유의하게 연관되어 있었으며(P = 0.032), 독립적인 전이 예측 인자로 확인되었다(HR = 3.365, P < 0.001). 또한, western blot 분석에서, NEK9와 EG5의 과발현이 대장암 세포주에서 유사분열 과정에서 중요하게 작용함을 확인하였고 NEK9-EG5 축이 pT3 대장암 환자의 전이 과정에 관련이 있을 가능성을 확인하였다. *ALK* 양성 NSCLC 환자에서는 (96명), 높은 HER3 발현이 생존율 저하와 상관관계가 있었으며, 특히 *EML4-ALK* 변이 1/2(V1/V2) 환자에서 더욱 두드러졌다. 이러한 상관관계는 ALK 억제제 투여 전 및 투여 후 조직에서 모두 유의미하게 관찰되었다 (P = 0.022, P = 0.004). Western blot 분석 결과, HRG1 유도에 의해 pHER3발현 되고 pAKT 및 pERK활성화가 입증되었다. ALK 및 EGFR 억제제를 병합한 치료는 *ALK* 양성 NSCLC 세포주에서 receptor tyrosine kinase 신호를 유의하게 감소시킴을 확인하였다. *ALK* 양성 NSCLC환자에의 (68명) T세포 밀도와 PD-L1 발현 분석 결과에서는, T 세포 아형과 PD-L1 간의 관계는 유의미하지 않았다. 그러나 spatial transcriptomic analysis에서는 PD-L1 양성 사례에서 *CD274* (PD-L1 암호화 유전자) 및 *PDCD1(PD-1 암호화 유전자)* 이 함께 발현되는 비율이 매우 적었으며, 반면 *CD68* (pan-macrophage) 및 *CD163* (M2-like macrophage)의 발현이 매우 높았다. 특히 *CD163* 이 발현되는 곳에서 *CD274* 발현 수준이 유의하게 높았으며, *PDCD1* 발현 수준은 PD-L1 양성 및 음성 사례 간에 큰 차이가 없었다. 이는 *ALK* 양성 NSCLC에서 PD-1 수용체와 PD-L1 리간드를 가진 세포 간의 직접적인 접촉이 포함되지 않을 수 있음을 의미하며, 이로 인해

면역 억제제의 제한된 효과와 관련이 있을 수 있다. 또한, 종양 관련 대식세포(TAM)의 높은 PD-L1발현에 비해 상대적으로 낮은 수준의 PD-1 양성 면역 세포 비율은 종양세포의 효과적인 면역 회피에 기여하는 데 제한적일 수 있다.

결론

본 연구 결과는 대장암에서의NEK9–EG5 축, *ALK* 양성 NSCLC에서HER3 발현 및 PD-L1 발현과 종양 미세환경의 상호작용을 이해하는 것이 환자의 맞춤형 치료 접근법에 새로운 길을 제공할 수 있음을 시사한다.